UNIVERSITÀ
DEGLI STUDI
DI PADOVA

UNIVERSITÀ DEGLI STUDI DI PADOVA

Dipartimento di Fisica e Astronomia

Scuola di dottorato in Fisica

XXVII CICLO

TESI DI DOTTORATO

SPATIAL CONFINEMENT OF BACTERIAL COMMUNITIES

Direttore della scuola: Prof. Andrea Vitturi

Supervisore: Prof. Giampaolo Mistura

Dottorando: Gaurav Jayaswal

FOUR BURNING CANDLES

In a room there were four candles burning. The ambiance was so soft you could hear them talking.

The first one said,

"I am **PEACE**, however nobody can keep me lit. I believe I will go out."
It's flame rapidly diminishes and goes out completely.
****

The second one says,
"I am **FAITH**. Most of all I am no longer indispensable, so it does not make any sense that I stay lit any longer."
When it finished talking a breeze softly blew on it putting it out.
****

Sadly, the third candle spoke in its turn.
"I am **LOVE**. I have not gotten the strength to stay lit. People put me aside and don't understand my importance. They even forget to love those who are nearest to them."
And waiting no longer it goes out.
****

Suddenly a child entered the room and saw three candles not burning. "Why are you not burning you are supposed to stay lit till the end."Saying this, the child began to cry.

Then

Fourth candle said,
"Don't be afraid, while I am still burning we can re-light the other candles, I am **HOPE**."

With shining eyes, the child took the candle of HOPE and lit the other candles, FAITH, PEACE and LOVE.
****

THE BOTTOM LINE IS:
The flame of Hope should never go out from our life and that each of us can maintain HOPE, FAITH, PEACE and LOVE.

Hope never abandons you. You abandon hope. Consult not your fears but your hopes and your dreams. Think not about your frustrations, but about your unfulfilled potential. Concern yourself not with what you tried and failed in, but with what it is still possible for you to do.

ADAPTED FROM SIR RICHARD FEYNMAN

"I would like to dedicate this thesis to my family members and my loving teachers for always guiding me and showing me the right path ... "

Abstract (English)

The subject of bacterial swimming has intrigued scientists for decades and recently there has been a growing interest in the study of collective swimming behavior of bacteria in a confined geometry. This thesis deals with a systematic experimental investigation of the density distribution of bacterial solutions of different concentration.

Two different types of bacteria, *Pseudomonas* and *E. coli*, have been used owing to their diverse propelling mechanism. *E. coli* behavior has been studied in detail, instead there are no reports in the literature regarding *Pseudomonas*, to the best of our knowledge.

The experimental set up consisted of two glass plates separated by spacers which define the confinement region. The separation distance ranged from 100 to 250 microns. The two plates were functionalized with bovine serum albumin (BSA) to avoid bacterial adhesion to the glass. The bacterial suspension was subjected to adjustment of buoyancy by addition of a density matching fluid like Percoll.

In agreement with previous studies, we found a significant enhancement of density close to the walls for both bacteria. This effect does not seem to be affected by either the separation distance or the solution concentration. These results were compared with those obtained by numerical simulations of self-propelled rod like particles which do not interact with each other apart from steric interactions. The preliminary data support the experimental outcome suggesting that steric interactions alone are sufficient to produce the observed enhancement effect.

Abstract (Italiano)

Il moto di batteri ha attratto gli scienziati da decenni e, ultimamente, c'è stato un crescente interesse nello studio del moto collettivo di batteri in geometrie confinate. Questa tesi descrive uno studio sperimentale della distribuzione di densità di soluzioni di batteri di concentrazione diversa confinate tra due pareti parallele.

Si sono usati due tipi di batteri, *Pseudomonas* ed *E. coli*, che presentano diversi meccanismi di propulsione. Il comportamento di *E. coli* è stato studiato in dettaglio, invece non ci sono lavori in letteratura riguardanti *Pseudomonas*, per quello che sappiamo.

L'apparato sperimentale consisteva di due vetrini separati da spaziatori che definivano la regione confinante. La distanza di separazione variava da 100 a 250 micron. I due vetrini erano funzionalizzati con albumina di serio bovino per evitare l'adesione dei batteri al vetro. Alla sospensione era stato aggiunto del Percoll per aggiustare la spinta idrostatica agente sui batteri.

In accordo con precedenti studi, abbiamo trovato un significativo aumento di densità in prossimità delle pareti per entrambi i tipi di batteri. Questo effetto non sembra essere influenzato né dalla distanza di separazione, né dalla concentrazione della soluzione. Questi risultati sono stati confrontati con quelli ottenuti da simulazioni numeriche di particelle auto-propellenti c he interagiscono solo mediante interazioni steriche. I dati preliminari supportano l'osservazione sperimentale suggerendo che le sole interazioni steriche sono sufficienti a produrre addensamento dei batteri alle pareti.

Acknowledgements

If I have seen further it is only by standing on the shoulders of giants.
~~ Sir Isaac Newton

I have spent an exciting and enjoyable three years learning period at University of Padova-Italy, largely due to the amazing people that I had the good fortune to associate with. The research described in this thesis is the culmination of years of hard work, and would not have been possible without the help of a number of people. I want to take this opportunity to thank them for their help and support.

I am grateful to my adviser Prof. Giampaolo Mistura, Dr. Matteo Pierno and Dr. Michele Merano for their advice, encouragement, and support over these years. Their enthusiasm for new ideas is infectious, and has helped to broaden my interest in Physics. I have enjoyed a lot learning from them.

My collaborators Prof. Enzo Orlandini, Prof. Andrea Squartini and Prof. Paolo Brun have helped me with their advice and suggestions, I am deeply grateful for that. My seniors Davide Ferraro and Emanuele Locatelli deserve special thanks for their help and advice during the starting days of lab. These two persons made all the instruments familiar to me and also to resolve all the paper/office work for my visa and stay permit.

One person in the optics group who cannot be thanked enough is Michele Merano. His help and advice in all experimental matters is indispensable. Besides being an excellent source of technical advice Michele is a wonderful person, who is always ready to go out of his way to help people. We had multiple opportunities to attend conferences together and Michele made an excellent company. We had lots of adventure trip, I will also remember the argument which we had with hotel personnel at San Jose and wonderful tour of Golden gate bridge. Thanks Michele

I was fortunate to have worked closely with Giorgio Delfitto (also known as uncle Gior-

gio and party man), Paolo Sartori, Enrico Chiarello, Siliva Varagnolo and Daniele Filippi. Enrico (Bill Gates of our group) has helped me understand a great deal about the algorithm of tracking software. His ability to think laterally was very helpful and inspiring. Especial thanks to Matteo Pierno for providing me in-depth knowledge of microscope and its parameters.

A significant portion of time in the bacteria measurement, corridor was spent in the company of Vera Russo. I am thankful to her for supplying the bacteria for my experiment. I would also like to thank to all the members of LAFSI, for providing homely atmosphere miles away from home. I wish all the members of LAFSI the very best in their endeavors. Especial thanks to Marco Bazzan, Stefano Vassanelli, Giovanni Mattei, Luca Salasnich and Nicolo Lo Gullo for their encouraging and helpful discussion.

I extend my heartfelt gratitude to all my school and college teachers, especially my previous supervisors Prof. A.V.Gopal, Prof. Mandar Deshmukh, Prof. Ramgopal Rao, Prof S.G.Prabhu, Prof. Vittorio Pellegrini and Prof. S.Dhar for implanting research quest in me. I feel highly indebted to them. I also thanks all my friends. I thoroughly enjoyed my stay at ESU residence with friends from all over the world.

A special thanks to Tanu Priya for her love, patience and unwavering support. She has transformed my life, and made it richer in countless ways. Writing thesis would have been impossible without her help and support. She was around me to share my frustrations and excitements, to support and to encourage. Thanks Tanu

I also take this opportunity to thank my parents, grand-parents, sisters and other family members for their love and encouragement. A special thanks to my late grand mother and late Ankit Jain. This work would not have been possible without their encouragement and from whose life I draw inspiration. My parents inculcated in me the ethics for hard work and I cannot thank them enough for that.

Finally once again I thanks Prof. Giampaolo Mistura for believing in me and giving an opportunity to do Phd in his esteemed research group. He was very helpful and kind during my entire stay, especially during my family problems. I will be highly indebted to him. Working with his group is like a blessing for me as I had multiple learning opportunities.

Thanks to God for providing me a such a nice research group. I am thankful to all the staff members of department of Physics, who have helped me some way or other during my stay. All these memories will remain in my heart throughout my life. I also thanks Fondazione Cassa di Risparmio di Padova e Rovigo (cariparo) for providing me fellowship.

Table of contents

Chapter 1

INTRODUCTION

Since its discovery and through past years "Active Matter" has become a paradigmatic topic in science. The term 'active' refers to the ability of individual units to move by transforming chemical energy, taken from the environment, into kinetic energy. Examples of such systems are bacterial suspensions, cell layers, flocks of birds, vibrated granular rods, fish schools, collection of robots and many more. The interaction with each other, and with the medium they live in, gives rises to highly correlated collective motion and mechanical stress. Active systems exhibit a wealth of intriguing non-equilibrium properties, including long range ordering, non-Boltzmann distributions, non-equilibrium order-disorder transitions, pattern formation on mesoscopic scales and unusual mechanical and rheological properties. All these new physical phenomena exhibited by active matter have attracted attention of many scientists and researchers working in the field of soft matter physics.

Amongst the different systems that belong to this class, bacteria become a model/ideal system for various reasons, as they provide a reproducible and reliable experimental system that displays a great variety of the features cited above. Bacteria are unicellular organisms, capable of self-reproduction and in many cases, motility (the biologists term for self-propulsion). A range of bio-mechanical mechanisms for motility are shown by different species of bacteria, the simplest of which is the swimming motion of species such as '*Escherichia coli*' and '*Pseudomonas*' (the same used for our study). Individual bacteria have helical flagella, each of which is forced to rotate by a biochemically powered motor.

Because of the chirality of these flagella, their clockwise and anticlockwise motion is inequivalent. One sense of rotation causes the flagella to form a coherent bundle which acts like propeller, resulting in a smooth swimming motion. Initiating the other sense of rotation causes the bundle to separate, with the result that the cell starts to rotate randomly. The canonical motion of bacteria then consists of periods of straight line swimming (called *runs*) interrupted by brief bursts of rotational motion (called *tumbles*).

Bacterial motility is one of the fundamental means of spreading infectious diseases, such as cholera and tuberculosis which pose serious health problems. Highly contagious diseases caused by microorganisms can lead to global and economical impacts such as pandemics. Li et al. [1] observed that bacterial tendency of accumulation to solid walls was argued to have important consequences on the infection process. Such an enhancement of bacterial density near solid walls has been studied in detail by Berke et al. [2]. This effect has been explained by hydrodynamic interactions that result in a reorientation of the swimmers in the direction parallel to the surfaces and an attraction of these aligned cells. However this explanation is still under debate, as a number of simulations suggest that this accumulation can be observed without the presence of hydrodynamics.

We have then decided to systematically study the confinement of various bacterial communities kept between two flat surfaces. In particular, we investigated the spatial distribution of two different types of bacteria, *E. coli* and *Pseudomonas*, by varying the density of the micro-swimmers and the lateral spacing between the two walls: These results are preliminary compared with the theoretical model developed by our theory collaborators (Prof.Enzo Orlandini Department of Physics-University of Padova and Prof. Davide Marenduzzo, Edinburgh University) based on extensive molecular dynamics numerical simulations on a coarse grained model of anisotropic self propelled particles.

The thesis is structured as follows: Chapter 1 describes the general properties of active matter, chapter 2 gives a brief introduction to bacteria (from the viewpoint of microbiology), chapter 3 illustrates the various models describing the motility behavior of bacterial communities in a confined geometry followed by the description of our coarse grain model. Chapter 4 describes material and methods of our studies along with experimental set-up and

characterization tools involved in our experiments. Chapter 5 shows the results of our confinement study and comparison of experimental results with theoretical model. Finally, the conclusions summarize the main results of this project and point out future prospects.

Chapter 2

Active Matter

Flocking birds, fish schools and quadruped herds are the most familiar and spectacular manifestations of collective motion. However, in nature there exist many other marvelous examples both in the living as well as in the non living world that exhibit a rich, coordinated behavior in systems that entail interacting and permanently moving units. Despite differences in the length scales, physical properties and cognitive abilities of constituent individuals. Their dynamics shows similar patterns of extended spatiotemporal coherence, suggesting universal features of collective motion. For these reasons, in recent years there has been a rapid growth of interest in modeling and measuring systems of *active matter*, i.e. collections of interacting particles with the capability of transforming energy into movement. A brief description of active matter along with its general properties will be presented in this chapter, together with some remarkable experiment on confinement studies.

2.1 Active Matter: Physical properties and examples

We define active matter as a collection of particles with internal degrees of freedom that have the ability to transform free-energy into work performed on the environment, resulting in directed motion [3]. The unifying characteristic of active matter is that it is composed of self-propelled active particles and the interaction of active particles with each other and with the medium they live in gives rise to highly correlated collective motion. Figure 2.1 shows

the collective behavior of some species that we commonly see in nature. Since active parti-

Fig. 2.1 A gallery of images showing collective behavior. (a) Fish school. (b) Three dimensional array of birds (flocking). (c) A herd of pengiun. (d) A rotating colony of ants. (e) Ordered motion of mosquito. (f) Collective motion in human crowds. *(Image source sciencereflection.com and guides.library.cornell.edu)*

cles can move autonomously, i.e. in complete absence of external forces, they are generally referred to as self-propulsion or self-propelled particles (SPP) [4]. Self-propelled particles are ubiquitous in nature, spanning an enormous variety of length scales. On the smallest length scales there are biological molecular motors, i.e. protein complexes that transform chemical energy, generally released by ATP hydrolysis, into mechanical work, and actin-myosin filaments, which are responsible for muscular contractions and which determine the mechanical properties of cytoskeleton in eukaryotic cells [5]. On the micrometer scale we

find not only living motile organisms but also artificial self-propelled particles. The former ones, such as cells or bacteria provided with flagella, are able to perform complicated non-reciprocal deformations that lead them to move in fluids which appear highly viscous given the small length scales [6]. The latter ones are designed to propel taking advantage of phoretic effects that become relevant at small scales in the presence of a non-homogeneous fluid [7, 8]. Typically, these self-phoretic particles generate through surface activity (e.g. catalysed chemical reactions, asymmetric heat release) a gradient of a field (e.g. concentration, temperature) which in turn induces phoretic motion [9]. Finally, on the macroscopic scale one can deal with all types of living organisms such as insects, fishes, birds, mammals and human crowds, but also man-made agents like queuing vehicles or self-organising mobile robots that give rise to collective motion characterized by impressively rich pattern formations [3].

2.2 General characteristics of active matter

Active matter exhibits a wealth of intriguing non-equilibrium properties, including emergent structures with collective behavior qualitatively different from that of the individual constituents, non-equilibrium order-disorder transitions, pattern formation on mesoscopic scales and unusual mechanical and rheological properties. Active matter is an out-of-equilibrium system in consequence of the different values of the intensive thermodynamic variables inside (or at the surface of) the particles with respect to the outside. As a result the energy input that enables motion is not due to any kind of flux at the boundaries but is distributed throughout the bulk of the system, taking place at the scale of each particle. This feature strongly differentiates active systems from other classes of driven systems such as sheared fluids or sedimenting colloids. Further, the direction in which each active particle moves is set by its own anisotropy and not by the direction imposed by an external field [10]. In other words, the action/direction of active matter is determined by internal states ("inherent dynamism") and/or environmental conditions ("induced dynamism"). They are not controlled by other instances (i.e. system administrator/leader), they operate on their

own. There is no geometry constraints in the movement of active matter, they can move in all dimensions, i.e. 1-D, 2-D or 3-D [10].

Another important features of active matter is that it often exhibits unusual mechanical properties, including strong instabilities of ordered state to small fluctuations and density fluctuations increase with the system size [11, 12]. Due to the energy absorption, active particles can undergo conformational changes that can influence the collective motion. Active particles take the initiative, i.e. they can start interaction with other particles or change their environment. The individual active particles are small compared to the system size, and it is assumed that individual particle actions do not change the system as a whole at once. Collective phenomena therefore arise from accumulated particle interactions [10].

Moreover, the interactions between the particles may usually occur on different spatial and temporal scales. This means that in addition to locally or spatially restricted interactions which may occur only at specific locations or if particles are closer, there is also a probability of global interaction, where all the particles are involved. Further, the timescale of interaction plays a significant role. Some interactions like in fish schools occur rather frequently, i.e. on a shorter timescale, others become effective only over a longer period of time like in flocking behavior of birds [10–12].

2.3 Biological examples of active matter

Many examples of active matter come from living/biological systems. One example is a dense bacterial suspension which contains a large concentration of bacteria dispersed in a liquid. In spite if its simplicity it displays novel collective behavior such as pattern formation [13] and turbulence [14] (see figure 2.2). Bacterial suspensions also show macroscopic orientationl order at high density. The origin of this ordering may come from excluded volume interactions between one bacterium and its neighbors, since the bacteria have rod-shaped bodies [16]. This is similar to polar liquid crystals [17], with the polarity defined to be the direction of swimming.

Another biological system of interest is represented by eukaryotic cells. These are bio-

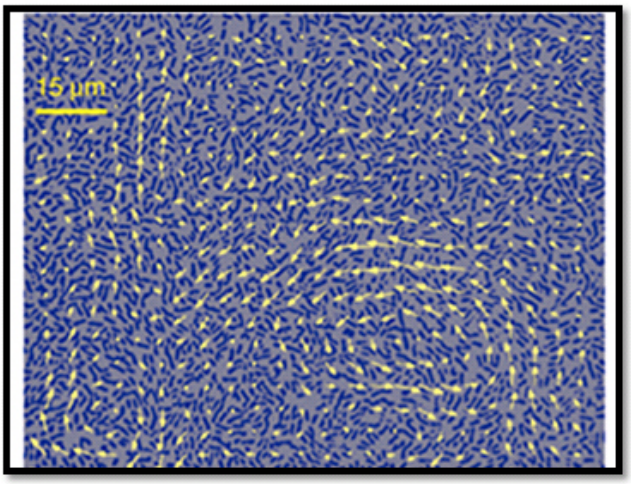

Fig. 2.2 Image of bacterial turbulence. Individudal bacteria are seen as short, dark rods, yellow arrows indicate the direction of the bacterial flow [15].

logical cells which come from most animals and plants tissues. Eukaryotic cells have long been known to be able to move in various media. For example, keratocyte cells found in the fishes have been observed to be able to crawl on a 2D glass substrate [18]. Another example is tumour cells which are able to swim inside a 3D tissue in vivo or polymeric gels in vitro [19]. While the mechanism for cell crawling has been explained (to a certain degree), the mechanism for cell swimming is still largely unknown. Such ability of the cells to move can be beneficial (e.g. in the case of wound healing [20]) or pathological (e.g. in the case of tumour cells migration to invade various parts of human body [21]).

From the experimental point of view, different systems of active matter require quite diverse experimental methods and their detection can vary considerably. For instance, fish school or bird flocks are not easily controllable and usually they can be observed for very brief periods in a year. For this reason, in recent years a great deal of experimental work in this field has been dedicated to the study of systems composed of bacteria [22, 23]. Practically, bacteria present many technical advantages including:

- Cells can be easily cultured in the lab.
- They have a fast growth rate.
- Easy to track.

- They can easily survive and can be stored in a lab.
- Experiments are highly reproducible.
- Experiments do not require complex equipment's.
- Experiments can be repeated in a very short span of time.

2.4 Confinement study of bacterial community

The quantitative study of the effects of the confinement on bacteria has become a highly studied topic. It finds application in the field of microbiology, water purification and bio medical research. Bacteria in a confined geometry interact with other bacteria, with walls and other obstacles. Three main contributions to these interactions can be distinguished:

a Volume exclusion: Prevents bacteria-bacteria interaction at short distances.

b Hydrodynamic interaction: Leads to alignment and attraction or repulsion depending on the propulsion mechanism of the bacteria.

c Thermal or intrinsic noise: Implies rotational diffusion of the swimming direction [7, 24].

In a remarkable experiment done by Di Leonardo et al. it was shown that it is possible to extract energy from the random motion of the bacterial bath. They experimentally demonstrated that a properly designed asymmetric rotor immersed in a random bacterial bath can be spontaneously set into desired motion [25]. The asymmetric microrotor is a gear with a sawtooth profile (see figure 2.3) whose center of mass is kept fixed at the center of the box [25, 26]. The propulsion mechanism is provided by the self-assembly of motile *E. coli* cells along the rotor boundaries. In the experiment, a micromotor was immersed in the bacterial bath.

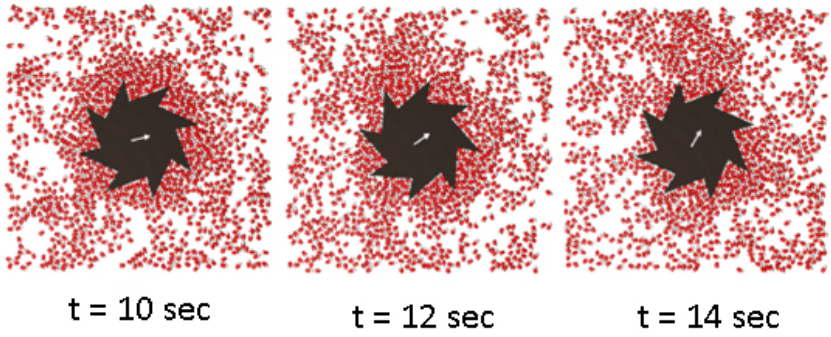

Fig. 2.3 Rotary micromotor in a bacterial bath. Snapshots are taken at three different times, t = 10, 12 and 14 sec [25].

The motor was free to rotate around its axis. The cell-boundary interactions produce a force and a net fluctuating torque on the gear motor, whose angular velocity is given by:

$$\Omega_g = K_g T_g$$

where T_g is the torque exerted by the bacteria on the gear whose rotational mobility is K_g. They found that the micromotor starts to move spontaneously under the effect of the pushing bacteria. The rotation thus produced can be understood by scrutinizing the collisions that take place between the bacteria and rotor boundary. When the bacteria collide with the rotor edge. They exert a force which can be realized by analyzing the projection of the propelling force on the surface of the rotor boundary (see figure 2.4). Bacteria coming from the left side with respect to the normal will leave the gear whereas bacteria coming from the right side get stuck at the corner of saw-tooth shaped rotor, exerting a net torque on the rotor. The torque exerted by the bacteria will thus move the micro-motor [25]. A net unidirectional motion was observed with a fluctuating angular velocity around a nonzero mean value. The instantaneous angular velocity ω of the motor as a function of time is shown in figure 2.5.

This provides an intriguing realization of the ratchet mechanism which was first discussed by Feynman [27]. In this experiment bacteria can be thought of as an analog of intrinsically off-equilibrium molecules. Asymmetric environments can be used to break the remaining spatial symmetries and allow the emergence of an ordered, reproducible motion that could serve as the driving mechanism for completely autonomous, self-propelling

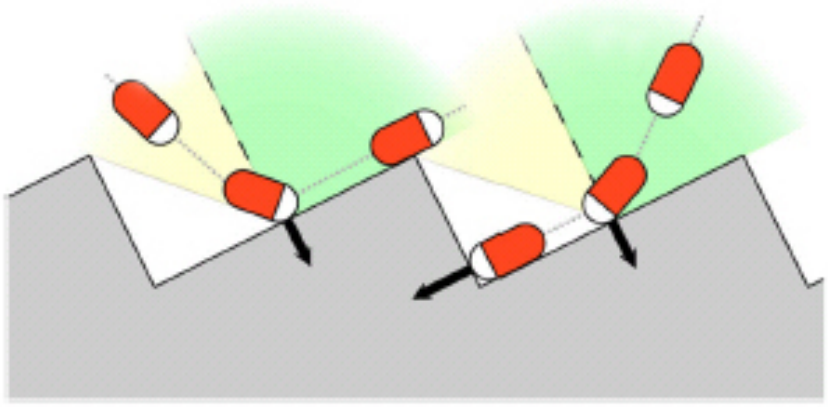

Fig. 2.4 Diagram showing the collision of a single bacterium with the rotor boundary. Arrows represent the forces exerted by the bacteria onto the rotor boundary [25].

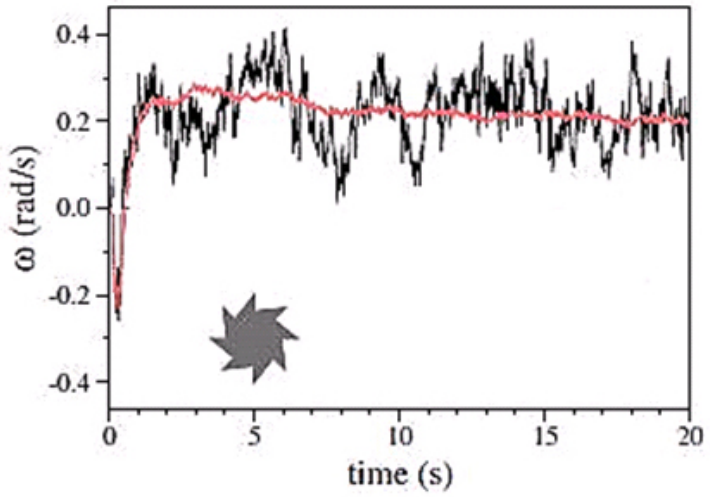

Fig. 2.5 Angular velocity ω of the micromotor as a function of time. The black line refers to a single run. The red line is the average over 100 independent runs [25].

micro-devices [25]. By using asymmetric object and self-propelled bacteria one can violate the time inversion symmetry. Once the time inversion symmetry is broken, a discontinuous spatial inversion symmetry gives rise to a spontaneous directed motion. From a thermodynamic point of view such irreversible dynamics reflects the constant entropy production [25].

The geometrically constrained interaction of bacteria with boundaries has also many other interesting properties. It has been shown that near solid surfaces, bacteria become

hydro-dynamically trapped and continue swimming along the surface [28]. Secondly, they accumulate near the surface, even without the involvement of chemo-taxis [1, 2]. It has been elaborated by a number of studies that this accumulation is dictated by physical interactions, including hydrodynamics, electrostatic, and Van der Waals interactions between the bacteria and the surface [29].

Rothschild and colleagues first measured the distribution of swimming bull spermatozoa between two glass plates separated by 200 μm. They observed that the distribution was non-uniform with an enhancement of density near the walls [30]. A few years later, H.Winet and his group observed similar results for human spermatozoa in glass tubes [31]. Recently some experimental and theoretical studies have discussed the effects of motility of micro-swimmers in confined geometry [32–34].

In one of the pioneering experiments on bacterial motion conducted by Berke et al. the phenomenon of density enhancement of the smooth swimming bacteria close to the walls was studied in detail. Figure 2.6 shows the representation of their experiment, wherein they measured the bacterial distribution between two microscopic slides separated by a fixed distance. To perform this experiment they used smooth-swimming *E. coli* a genetically

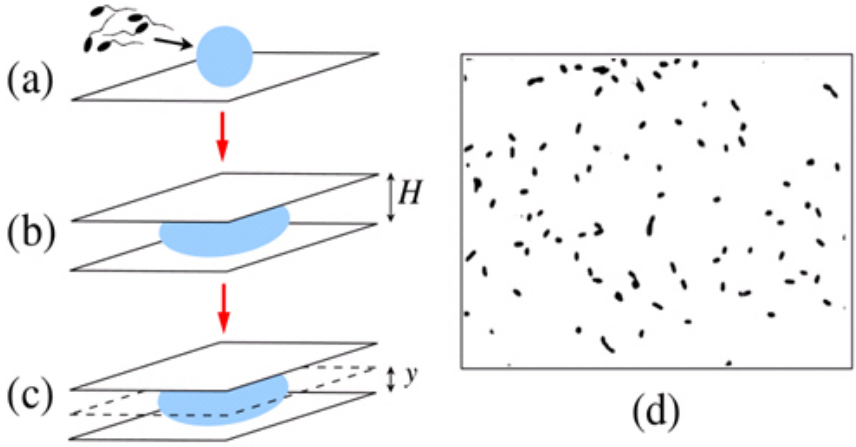

Fig. 2.6 A diagram of Berke et al. experiment. (a) Smooth-swimming *E.coli* cells. (b) The cell solution between two glass plates (separated by distance H). (c) The distribution of swimming cells as a function of the distance y from the lower surface. (d) Cell distribution [2].

modified mutant of *E. coli* in which the tumbling phase is suppressed. Henceforth, these

bacteria tend to swim only in one direction. They measured the bacterial distribution between two walls by using phase contrast microscopy, which focuses only on those bacteria which lie on the focal plane within the margin defined by the depth of field of the objective (equal to $4.3\mu m$ in the experiment). They recorded the image sequences by using a Nikon digital camera from bottom to the top wall with step size of 10 μm. Figure 2.7 shows the experimental results, where the density enhancement of bacteria close to the surfaces is evident. A semi quantitative explanation was given by the same authors. They suggested that hydrodynamic interaction in the dipole approximation (valid for distances much longer than the length of the swimming cells), result in a reorientation of the swimming cells in the direction parallel to the surfaces and an attraction of the aligned cells by the nearest wall [2]. Hydrodynamic interactions have been considered as the major contributor for the density

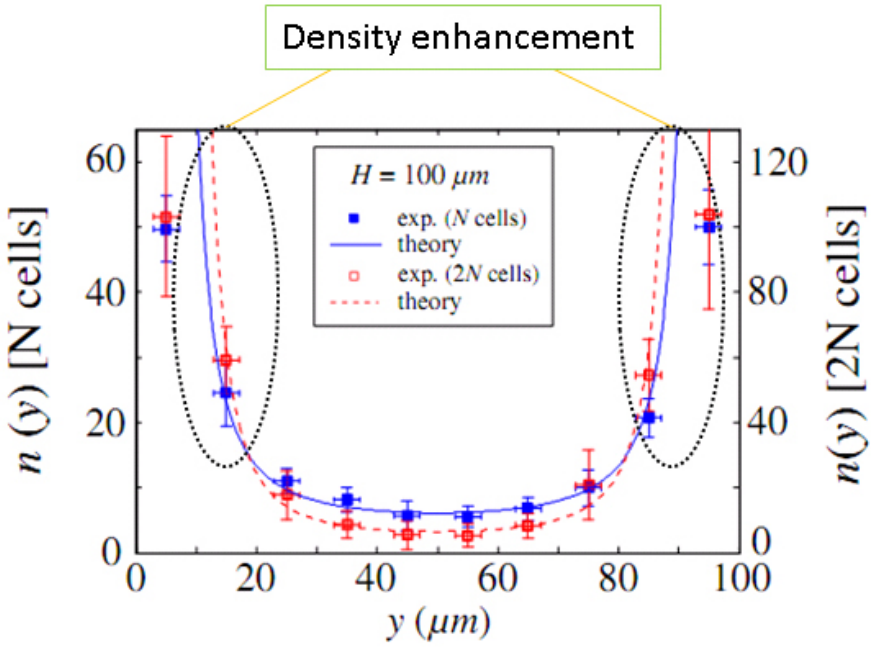

Fig. 2.7 Experimental results of Berke et al. The graph of the number of bacteria vs distance between the two walls. The y coordinate goes from 0 (corresponding to the bottom wall) to 100 (corresponding to the upper wall). The blue and red dots represent the experimental data for different densities whereas solid and dot lines represent the curves predicted by the theoretical model [2].

enhancement of swimming bacteria near the surface [35, 36]. Hydrodynamic interaction along the surface keeps a forward swimming bacteria parallel to the surface at a distance

comparable to the bacterial body width following a circular trajectory [37] but Elgeti et al. showed that this is only true for the bacteria with high Péclet number (P_e). For bacteria with low (P_e) (see chapter 4), other mechanisms of surface accumulation may dominate, such as the alignment of rod-like bacteria parallel to a wall or crowding [35, 38]. They provided an analytical solution for a system of a self-propelled Brownian spheres. They found that self-propelled spheres yield a denser accumulation near the walls as compared to self propelled rods. They concluded that simple self-advection Brownian dynamics of spherical particles is sufficient to generate strong surface adhesion [35, 38].

In the study performed by Li et al. [39] it was shown that the accumulation of swimming bacteria near the surface is due to the frequent collisions of the swimming bacteria with the surface, causing them to align parallel to the surface as they continually move forward. They demonstrated that accumulation of swimming bacteria near the surfaces depends on the swimming speed and size of the bacteria. Longer and faster moving bacteria accumulate more near a surface than the shorter and the slower ones. They have also shown that accumulation of swimming bacteria within a few micrometers from a surface is highly relevant to bacterial adhesion and biofilm formation. The closer a bacterium is to a surface, the higher is its chance to adhere to the surface as shown in figure 2.8.

Howard Stone's group describes the phenomenon of density enhancement of bacteria near the solid surface as more like a trapping effect rather than an attraction effect. Force-free and torque-free swimming lead to a hydrodynamic trapping of the cells close to the surface. This trapping is probably responsible for the extended period of time during which swimming bacteria are observed to remain near surfaces, which enhances the probability of cell adhesion to substrates [40].

It has been observed that also the materials of the confining geometry affect the bacterial distribution. Diluzio and Whitesides have shown that when bacteria are confined between two different interfaces, i.e. between agar gel and PDMS, bacteria swim closer to the agar surface than to the PDMS surface and also the duration of swimming is longer near the agar surface as compared to PDMS surface. Thus, the choice of materials guides the motion of bacteria in confined geometry. They fabricated a micro-channel as shown in figure 2.9

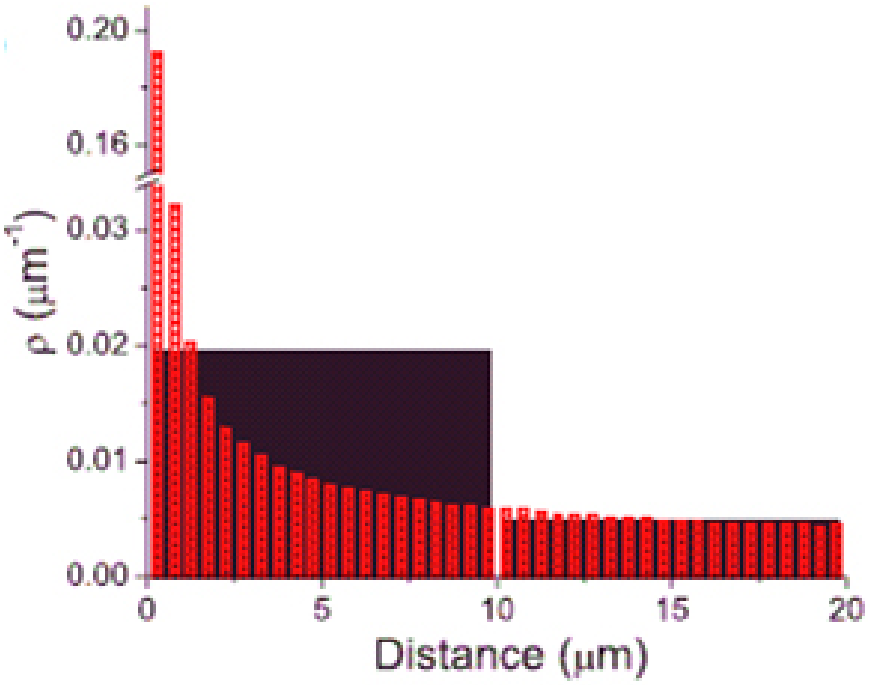

Fig. 2.8 (The probability distributions of bacteria as a function of the distance from the surface of the wall.) [39].

[34]. Oxidized PDMS film was placed on the agar. The film sealed conformally to the agar substrate and formed micro-channels in which bottom agar surface formed the floor of the channel and the oxidized PDMS film formed the sidewalls and ceiling. They observed preferential movement of the bacteria only when agar was used either for floor or ceiling of the micro-channel. When the floor and ceiling was composed of oxidized PDMS, the bacterial motility was hindered. Since agar is a porous gel with a wide distribution of pore sizes. They concluded that bacteria experience less resistance to their movement when they swim close to porous agar surface rather than when they swim close to the non-porous oxidized PDMS surface [34]. Finally, not only the nature of the walls but also the shape has a significant impact on the motility of the bacteria as demonstrated in an experiment conducted by Hulme et al. They fabricated a channel of suitable shape (ratcheting micro-channel of 1.5 μm in height) that directs the motion of *E. coli* in one direction due to their interaction with the walls. No external pumping or flow is involved and instead motile bacteria propel themselves through the channel. In this experiment the lateral and top walls

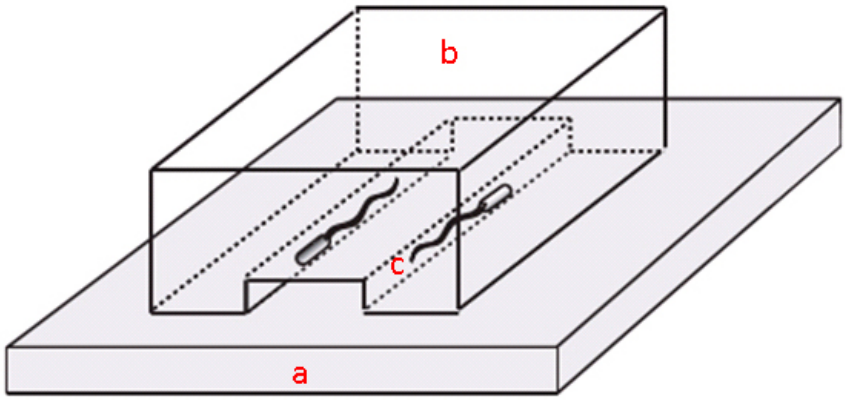

Fig. 2.9 An experimental set-up of Whitesides et.al, (a) is the agar substrate, (b) is the PDMS wall and (c) is micro channel into which *E. coli* swims. [34].

were made of PDMS and bottom wall was made of Agar [41]. Figure 2.10 shows a single ratchet as well as the trajectories of the bacteria swimming inside the ratchets. The same

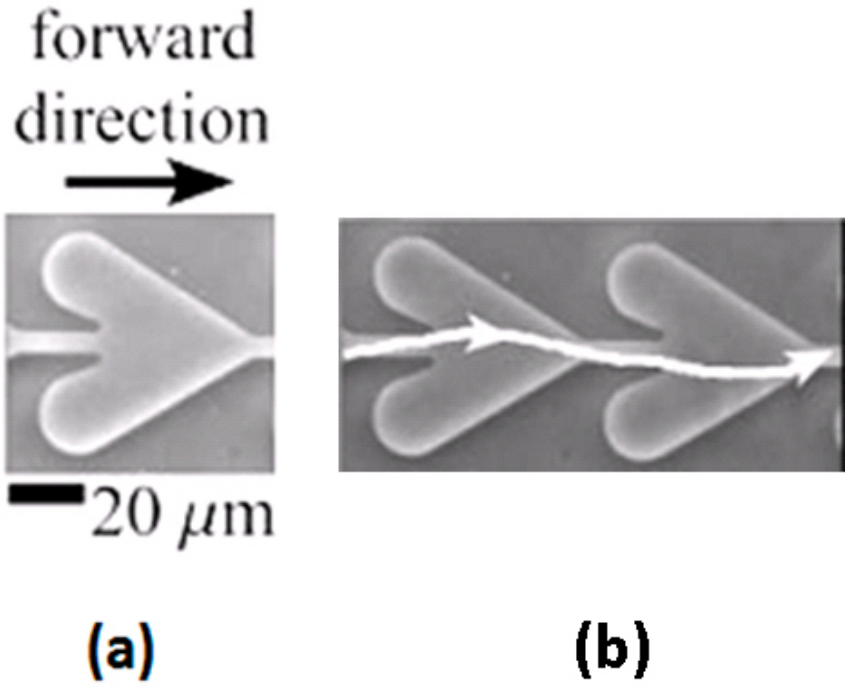

Fig. 2.10 (a) Represent a single ratchet. (b) Represent the cell trajectory of swimming bacteria inside the retchets [41].

group also demonstrated that the unidirectional movement in ratchets allows trapping and concentrates bacterial cells in microchannels. When the ratcheting channels lead to a dead end, bacterial cells swim to the end of the channel and become trapped [41].

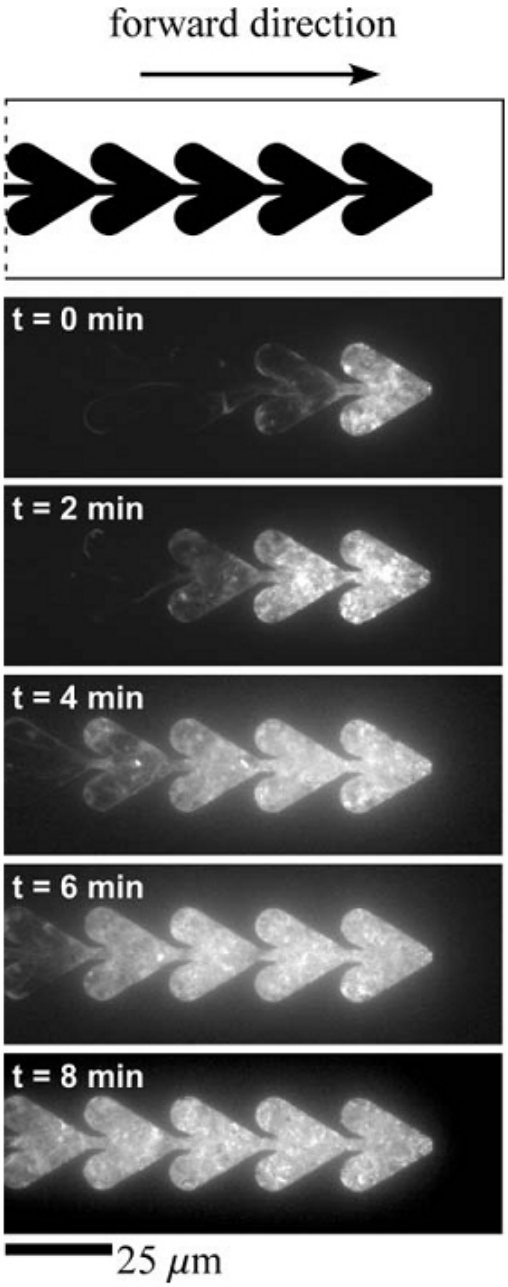

Fig. 2.11 Time-lapse images of fluorescent *E. coli* trapped and concentrated in bacterial ratchets [41].

Figure 2.11 shows a series of florescence micrographs of bacterial cells trapped at the end of a ratcheting microchannel over a period of 8 minutes. Over this period, more and more bacteria accumulate at the end of the channel so that the final ratchet becomes packed with bacterial cells (see figure 2.11). In addition to the unidirectional guidance of swimming bacterial cells, the ratcheting microchannels can be used for separating motile from non-motile bacteria or live motile bacteria from dead bacteria. It may thus be possible to use the ratchets to isolate motile bacteria from the environment. Because the ratchets can cause the accumulation of bacterial cells at high concentration at the end of a channel, the ratcheting microchannels may also be useful for studying bacterial phenomena that depend on the concentration of a population (like quorum sensing).

These results open the possibility to further investigate the role of geometrical shapes in regulating and sorting the population of the active swimmers. This has become a hot topic of research and a lot of studies have gone into understanding this phenomenon and much remains to be explored and investigated.

Chapter 3

Introduction to Bacteria

Bacteria are unicellular entities ubiquitous in nature known to survive in the harshest environments, thus forming the biggest chunk of biomass on this planet. Although bacteria are millions of years older than mankind, we are closely related in terms of storing genetic information and carrying out life essential processes. Many of us know of bacteria as germs, microscopic creatures that can invade our bodies and make us sick. In actuality, they also perform vital functions in the world we live in, for example, nitrogen fixation in soil or decomposition of biological waste. Understanding the phenomena of how bacteria thrive and multiply has intrigued researchers for decades. It has had and will continue to have a great significance in the field of biology and in general human welfare.

This chapter gives a brief introduction to bacteria, mainly *Escherichia coli* (*E. coli*) and *Pseudomonas*, which have been employed in our research. The general characteristics of both bacterial species, including growth, bacterial categories, morphology, habitat, and motility are discussed in this chapter. Finally, the mechanism of cellular motility and chemical signaling which enable cells to sample the environment and swim towards attractants or away from chemical repellents are also presented in this chapter.

3.1 Anatomy of Bacteria

The field of microbiology was formed shortly after the advent of the single lens optical microscope in 1687 by Antoie van Leeuwenhoek [42]. Leeuwenhoek is considered as the father of microbiology and the first microbiologist to observe and analyze swimming bacteria [43]. Leeuenhoek examined droplets of rain water underneath a microscope and noted that they contained miniature creatures which he called "*animalcules*". Bacteria are microscopic living organisms, usually unicellular (as shown in figure 3.1) and are omnipresent. Their small size, ability to rapidly reproduce and survive in diverse habitats/modes of existence make bacteria the most abundant and diversified group of organisms on the Earth. A gram of soil typically contains about 40 million bacterial cells. A milliliter of fresh water usually holds about one million bacterial cells. Planet Earth is estimated to hold at least 5 nonillion (5×10^{30}) bacteria [44, 45]. Bacteria can be dangerous, such as when they cause infection, or beneficial, as in the process of fermentation (such as in wine). A bacterial cell

Fig. 3.1 A micro-graph showing bacteria in water.

is different from the cells of plants and animals as bacterial cells have no nucleus and other organelles which are present in animal and plant cells. Bacteria have pili, flagella, and a cell capsule (most of them), unlike animal or plant cells. Figure 3.2 shows the difference between the bacterial cells with respect to plants and animals cells. Since bacterial cells have no nucleus, cell organelles are scattered in the cytoplasm including the genetic materials. There is only a thick cell wall which encloses all the organelles and gives the proper shape

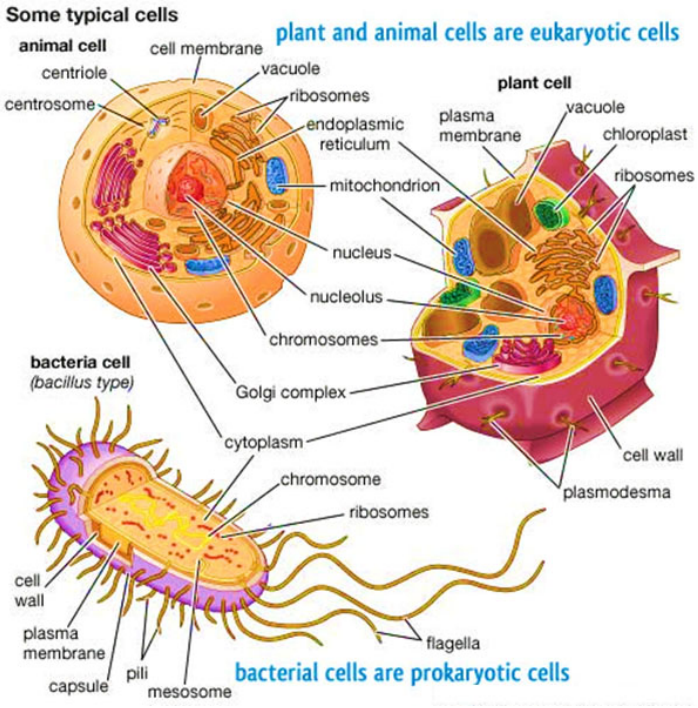

Fig. 3.2 Schematic diagram showing the difference between bacterial cells with animal and plants cells. *Image source Britannica encyclopedia 2007*

to the bacteria [45, 46]

A bacterial cell includes:

- Basal body: This anchors the base of the flagellum, which allows them to rotate.

- Flagella: These are the organs responsible for the motility. Flagella are composed of flagellins (proteins) that make up the long filament. This filament is connected to a hook and rings that anchor the flagella to the cell wall. Flagella may be up to 20 μm in length. Some bacteria possess a single polar flagellum (monotrichous), others have several polar flagella (lophotrichous), some species have several flagella at each end of the cell (amphitrichous) and others have many flagella covering the entire cell surface.

- Pili: These surface appendages come in distinct forms having distinct purposes. Pili may also provide antigenic determinants (e.g. the M protein of S. Pyogenes).

- Capsule: It is the surface layer mainly composed of high molecular weight polysaccharides. If the layer is strongly adherent to the cell wall, it is called a capsule; otherwise, it is called a slime layer. These layers provide resistance to phagocytosis and serve as antigenic determinants. The production of capsules is genetically and phenotypically controlled.

- Plasma membrane: It helps in transportation of chemicals and nutrients within the cells. Substances can pass through the membrane (permeable). It is located within the cell wall.

- Cytoplasm: A gelatinous substance inside the plasma membrane. Genetic material and ribosomes lie inside.

- Ribosomes: This is where proteins are formed (synthesized). Ribosomes are small organelles made up of RNA-rich granules [47, 48].

The bacteria cells have a chemically complex envelope. The cell envelope consists of a tightly bound three layered structure: the outermost glycocalyx followed by the cell wall then the plasma membrane, which act together as a protective unit. Bacteria can be classified into two groups on the basis of the differences in the cell envelopes and the manner in which they respond to the staining [49]. The gram staining technique was developed by Christian Gram in the year 1884. Bacteria smear is heat fixed on a glass slide which is then dipped in a solution of crystal violet for a minute. All types of bacteria pick up purple coloration. The stain is fixed by dipping the side in 0.5 % iodine solution for a minute. The slide is then kept on a polar organic solvent like alcohol or acetone for 10-30 seconds. Some bacteria retain a blue or purple stain. They are called Gram positive. Those losing the stain are instead designated as Gram negative. The slide is counter stained with Safranin for 20-30 seconds. Gram negative bacteria pick up the pink counter stain while Gram positive bacteria come to have both purple and pink stain. The difference between Gram positive and Gram negative is due to difference in lipid content of their walls as shown in figure 3.3. In Gram positive bacteria the wall has very little lipid content (1-5 %) therefore very little stain leaks out of their walls in organic solvent. In Gram negative bacteria, the wall

has high lipid content (20-30 %) which dissolves in organic solvent taking out the stain along with it. Gram negative bacteria have an extra lipopolysaccharide layer which is absent in Gram positive bacteria. Gram positive bacteria have a rigid cell wall due to high percentage (80 percentage) of peptidoglycan compared to low percentage (3-12 %) in Gram negative bacteria. Gram negative bacteria are capsulated which makes them virulent, while the Gram positive bacteria are noncapsulated. Only a few forms of Gram positive bacteria are pathogenic and may produce exotoxins. e.g. *Bacillus Clostridium, Lacobacillus, Streptococcus, Leuconostoc, Staphylococcus, Corynebacterium.* Most forms of Gram negative bacteria are pathogenic and may produce endotoxins. e.g. *E. coli, Salmonella, Acetobacter, Azotobacter, Vibrio, Agro bacterium, Pseudomonas, Shigella* [50, 51].

Gram negative species are often more resistant to antibiotics, detergents and dyes whereas Gram positive species are more sensitive and susceptible to chemical attacks [52, 53].

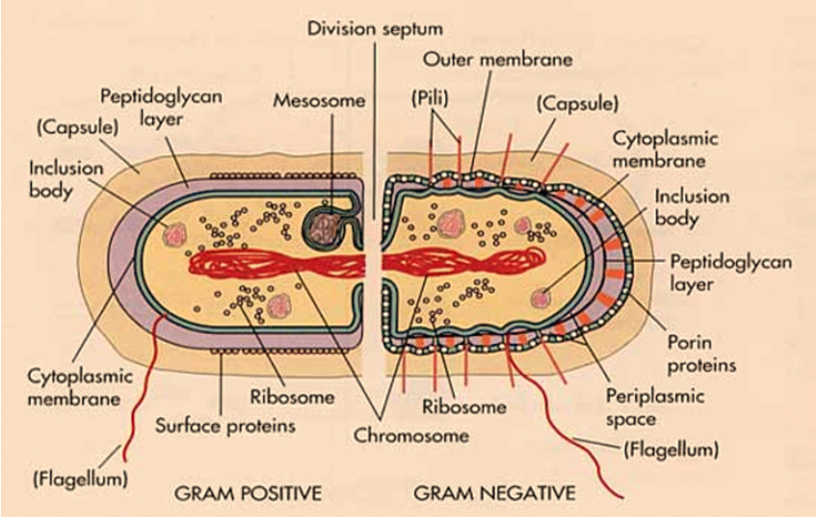

Fig. 3.3 A schematic diagram of the cellular structure of Gram positive and Gram negative bacterium. *Image source digitalproteus.com*

3.2 Types of Bacteria

Bacteria display a wide diversity of shapes and sizes. Bacterial cells are about one tenth the size of eukaryotic cells and are typically 0.5 μm to 5.0 μm in length. However, a few species

like *Thiomargarita Namibiensis* and *Epulopiscium Fishelsoni* — are up to half a millimeter long and are visible to the naked eye, e.g. *E. Fishelsoni* reaches 0.7 mm in length. Among the smallest bacteria are members of the genus *Mycoplasma*, which measure only 0.3 μm, as small as the largest viruses. Bacteria can have different shapes as shown in the figure 3.4 [54].

- Spherical (like a ball): These are usually the simplest ones. Bacterial with this shaped are also known as cocci . e.g. *Streptococcus*

- Rod shaped: These are known as bacilli, e.g. *E. coli*. Some of the rod-shaped bacteria are also curved which are known as vibrio. e.g. *Salmonella*, *Lactobacilli*,

- Spiral: These are known as spirilla. If their coil is very tight they are known as spirochetes. e.g. *Treponema Pallidum*

More recently, bacteria were discovered deep under the Earth's crust that grow as long rods with a star-shaped cross-section. The large surface area to volume ratio of this morphology may give these bacteria an advantage in nutrient-poor environments. This wide variety of shapes is determined by the bacterial cell wall and cytoskeleton, and is important because it can influence the ability of bacteria to acquire nutrients, attach to surfaces, swim through liquids and escape predators.

Depending on the environment, bacteria can be classified as:

- Aerobes (aerobic bacteria): Bacteria under this category can grow only in the presence of oxygen. Some strains may cause serious problems to buildings and infrastructure like corrosion, fouling, problems with water clarity, and bad smells. e.g. *Staphylococcus species*, *Streptcoccus species*, *Myobacterium tuberculosis*, *Bacillus*, *Nocardia* and *Pseudomonas aeruginosa*.

- Anaerobes (anaerobic bacteria): They can grow only in the absence of oxygen. In human-beings, they are most commonly found in the gastrointestinal tract. They are responsible for causing gas gangrene, tetanus and botulism. Most dental infections

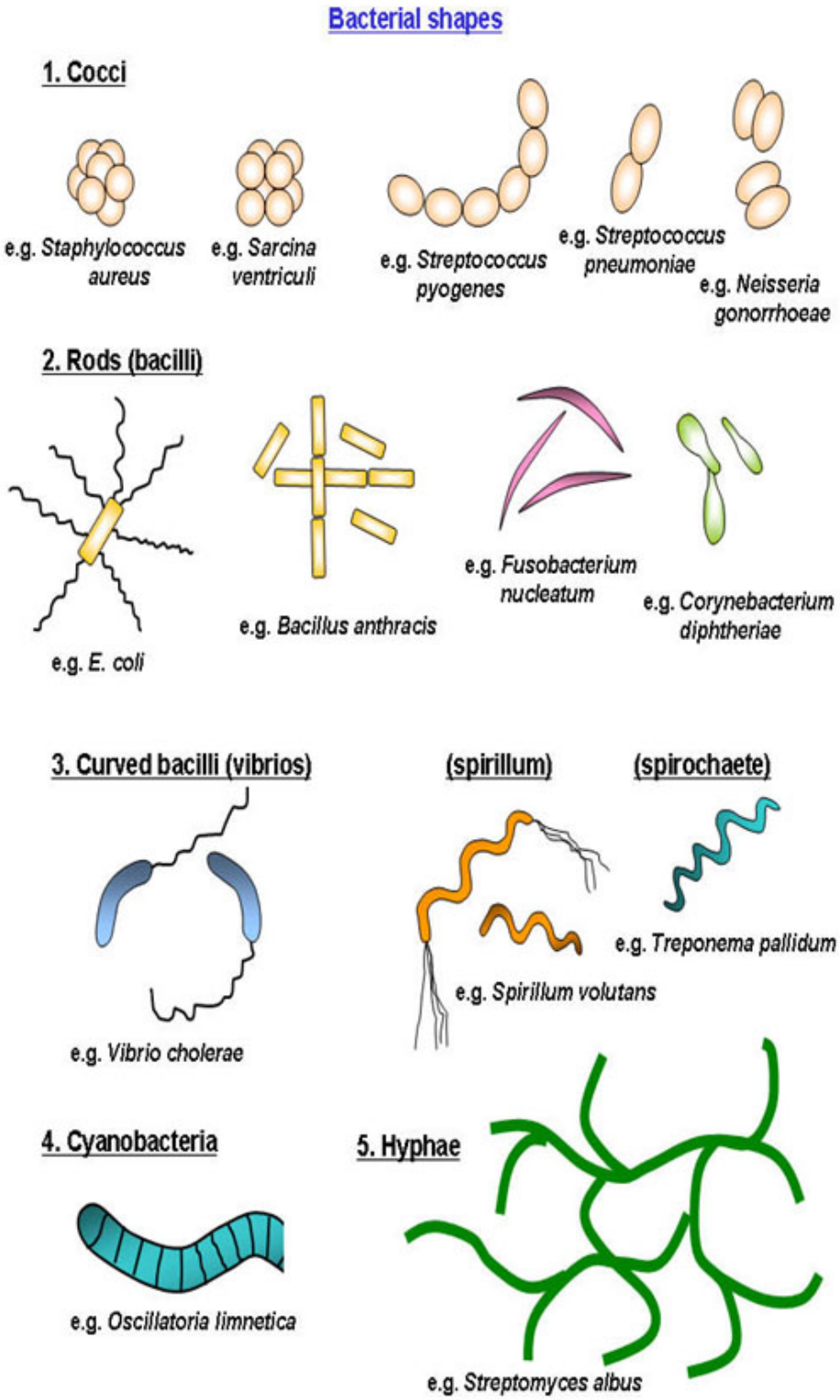

Fig. 3.4 A schematic diagram showing the different shapes of bacteria which exist in nature. *Image source tabletsmanual.com*

are caused by this type of bacterium. e.g. *Clostridium tetani*, *Clostridium botulinum* (which mainly causes food poisoning) , *E. coli* and *Actinomyces*.

- Facultative anaerobes (facultative anaerobic bacteria): These types of bacteria thrive in environments with or without oxygen. However, when both options are given, they prefer to use oxygen for respiration. They are mainly found in soil, water, vegetation and some normal flora of humans and animals. e.g. *Salmonella*.

- Mesophile (mesophilic bacteria): Human bacterial infections are mainly caused by mesophilic bacteria because these types of bacteria thrive in moderate temperatures i.e. $(30-35^{o}C)$, which are very much similar to the moderate (average) human body temperature. e.g. *Thiobacillus novellus*, *Staphylococcus aureu*, *Streptococcus pyrogenes*, and *Clostridium kluyveri*.

- Extremophiles (extremophilic bacteria): These bacteria survive in extreme conditions which can be difficult for most of the life forms (including man-kind). There are several different types of extremophilic bacteria, depending upon the kind of extremes they can tolerate:

  - Thermophiles (thermophilic bacteria)- Comparison with other strain of bacteria the thermophiles can sustain high temperatures like that of boiling water. Henceforth it takes longer to kill them in boiling water with respect to other bacteria. e.g. *Pyrolobus fumarii*.

  - Halophiles (halophilic bacteria)- They can survive only in a salty environment such as saltine lakes. e.g. *Halobacteriacea*.

  - Acidophiles (acidophilic bacteria)- Acidophiles can only thrive in acidic environments. e.g. *Cyanidium Caldarium*, and *Ferroplasma sp* can tolerate an environment with an acidity of pH 0.

  - Alkaliphiles (alkiliphilic bacteria)- These category of bacteria can live in alkaline environments. e.g. *Natronobacterium*, *Bacillus firmus* can all tolerate up to pH 10.5.

- Psychrophiles (psychrophilic bacteria)- These bacteria can only thrive at very low temperatures, i.e. in glaciers and cold region e.g. *Psychrobacter* [54, 55].

Mode of nutrition of bacteria varies among different species. Two main classes can be distinguished:

- Heterotrophic bacteria: These kind of bacteria eats other organisms. For instance *Saprobes*, which eat the decomposing flesh of dead organism material. Some of these parasitic bacteria kill their host, while others help them.

- Autotrophic bacteria: These types of bacteria can synthesize their own food by photosynthesis: bacteria use sunlight, $C0_2$ and water to produce their food (such strain of bacteria are called photoautotroph). Another possibility is through chemosynthesis: bacteria use $C0_2$, water and chemicals such as ammonia to synthesize their food (nitrogen fixers). They are commonly found in roots of leguminous plants [54–56].

3.3 *E. coli* and *Pseudomonas*

E. coli is predominately found in the human gut and digestive track. In microbiology, *E. coli* is regarded as the ideal microorganism for laboratory studies and is extensively used for research purposes. *E. coli* is a genus of "*Escherichia*" and belongs to the family of "Enterobacteriaceae". It was first identified by Theodor Escherich, after whom it was later named. Despite *E. coli* being one of the simplest form of life, it has demonstrated remarkable sophistication in terms of genetics compositions, the regulatory sensory system, cellular functionality and motility [57]. *E. coli* cells are extremely robust and resourceful in adverse biological environments and, above all, *E. coli* is also experimentally easy to handle and maintain in labs.

E. coli cells are rod-shaped having length (end to end) of 2-3 μm and 1.0 μm in diameter with hemispherical end caps often described as a prolate spheroid as shown in figure 3.5. They belong to the Gram-negative family and they are classified as anaerobes. Individual *E. coli* cells have approximately 4-6 flagella, each flagellum is 5 μm in length and

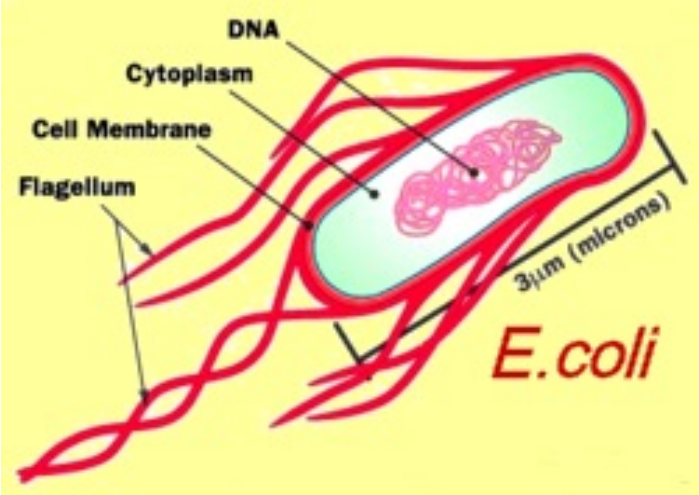

Fig. 3.5 A schematic diagram of *E. coli*. *Image source qmrawiki.msu.edu*

approximately 25 nm in diameter [49, 53].

Majority of *E. coli* strains are harmless but a few of them can cause serious food poisoning and bloody diarrhea leading to kidney failure especially in young children or in people with weak immune system. The *E. coli* infection is mostly due to consumption of contaminated food or water, contact with an effected person or contact with animals that carry the bacteria.

The harmless strains are part of the normal flora of the gut, and can benefit their hosts by producing vitamin K2, and preventing colonization of the intestine with pathogenic bacteria. The most commonly *E. coli* strain are (a). Clifton wild type, (b). W3110, (c). DH5α and (d). Dam-Dcm strain.

Pseudomonas is a member of the *Gamma Proteobacteria* class of bacteria. It is a genus of Gram-negative bacteria and belongs to the family of *Pseudomonadaceae*. They are aerobic, rod-shaped, with one or more polar flagella, responsible for motility as shown in figure 3.6. The best studied species is *Pseudomonas aeruginosa* (*P. aeruginosa*), which was used in our experiment purposes. Like other members of the genus, *P. aerugiosa* is a free living bacterium, commonly found in soil and water. However, it occurs regularly on the surfaces of plants and occasionally on bodies of animals. In fact *P. aeruginosa* is the epitome of

an opportunistic pathogen of humans. The good thing with this bacterium is that it almost never infects unconnected tissues [58, 59].

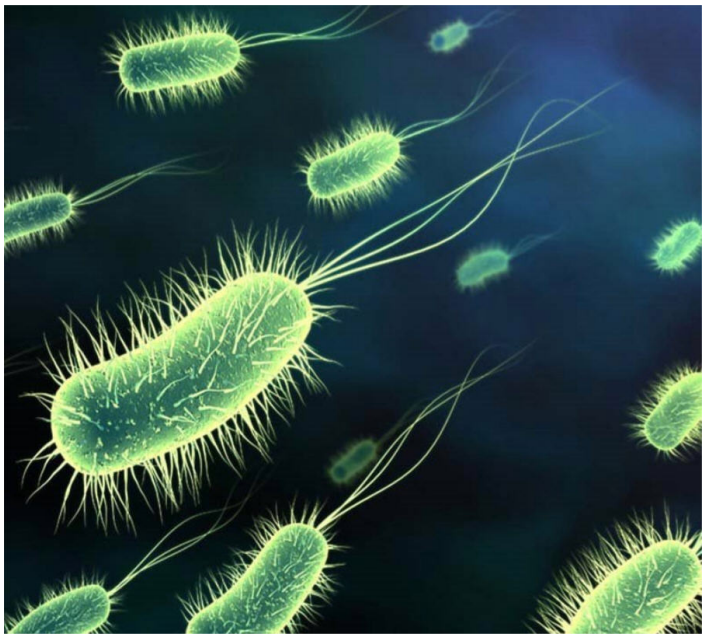

Fig. 3.6 A schematic diagram of *Pseudomonas*. *Image source thesilveredge.com*

Pseudomonas species have lengths (end to end) of 1.5 to 3 μm and 0.5 to 0.8 μm in diameter. Almost all strains are motile by means of a single polar flagellum. The bacterium is ubiquitous in soil and water. It can also grow in the absence of 0_2 [60]. Other characteristics are:

- *P. aeruginosa* has very simple nutritional requirements. It is often observed "growing in distilled water", which is evidence of its minimal nutritional needs. In the laboratory, the simplest medium for growth of *P. aeruginosa* consists of acetate as a source of carbon and ammonia sulfate as a nitrogen source.

- *P. aeruginosa* possesses the metabolic versatility for which *Pseudomonas* are so renowned. Organic growth factors are not required and it can use more than seventy-five organic compounds for growth.

- The optimum temperature for growth is 23^oC and it is able to grow at temperatures as high as 42^oC.

- They are tolerant to a wide variety of physical conditions, including temperature. They are resistant to high concentrations of salts and dyes, weak antiseptics and many commonly used antibiotics.

- *P. aeruginosa* has a predilection for growth in moist environments, which is probably a reflection of its natural existence in soil and water. Figure 3.7 shows the strain of *P. aeruginosa* inside water.

Fig. 3.7 *P. aeruginosa* as observed under an optical microscope.

Some of the *Pseudomonas* species like *P. borbori, P. straminea* and *P. fluorescens* may cause urinary tract infections, respiratory system infections, dermatitis, soft tissue infections, bacteremia, bone and joint infections, gastrointestinal infections and a variety of systemic infections [61]. People who wear contact lenses can get serious eye infections if the bacteria get into their contact lens solutions. *Pseudomonas* species are also responsible for the spoilage of milk even after the process of pasteurization.

3.4 Bacterial Growth

All bacterial species regardless of cellular category (Gram positive/negative) grow and multiply by binary fission, a process of asexual reproduction in which a single mother cell di-

vides into two approximately equal length daughter cells. Each daughter cell is genetically identical, as schematically shown in figure 3.8.

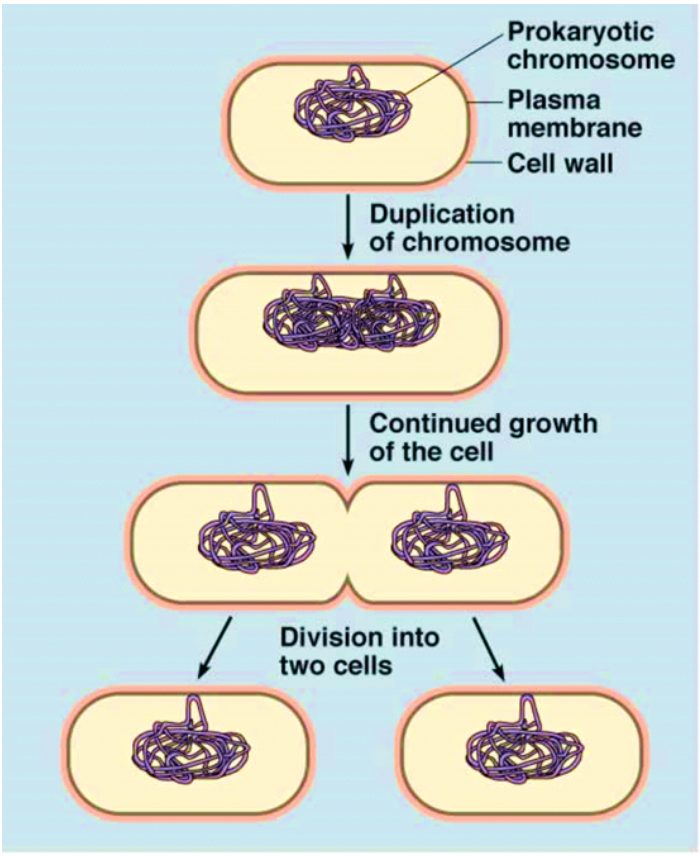

Fig. 3.8 A schematic diagram of the binary fission process of a rod-shaped bacterium. *Image source meritnation.com*

The time it takes for one mother cell to divide into two daughter cells is known as the generation time g (also known as doubling time), which is strongly dependent on the bacterial growth conditions. The progressive doubling of the cells results in a continuously increasing population referred to as exponential growth. Thus mother cell divides into two independent daughter cells, these two daughter cells subsequently divide into four daughter cells and so forth [45, 62].

When a bacterium is inoculated in a medium, it passes through four growth phases which are dependent on the growth conditions. The growth of bacterium reproducing by binary fission can be plotted as the logarithm of the number of viable cells (i.e. living cells) versus the incubation time, and the resulting curve is shown in figure 3.9.

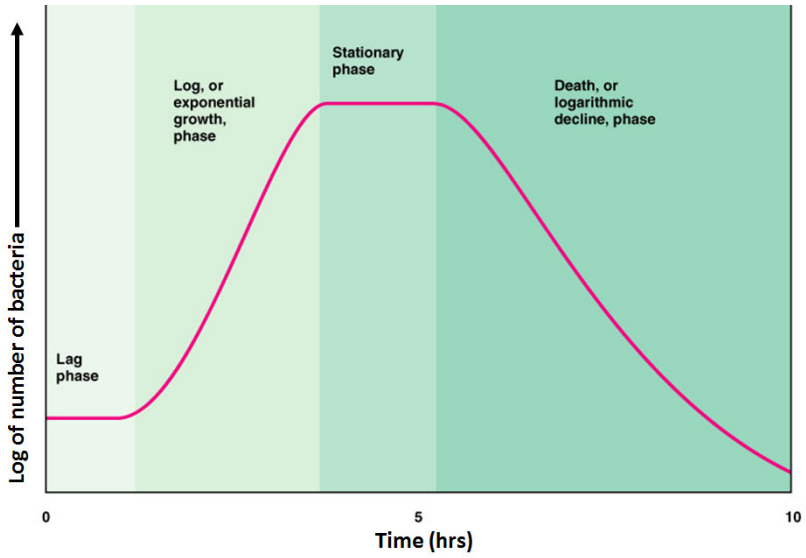

Fig. 3.9 A schematic diagram of different growth phase of bacterium. *Image source midlandstech.com*

Four distinct phases can be identified:

1. *Growth Phases or Lag Phase*: In this phase there is an increase in cell size but not multiplication. Time is required for adaptation (synthesis of new enzymes) to new environment. Enzymes and intermediates are formed and accumulate until they are present in concentration that permits growth to start. Antibiotics have little effect at this stage.

2. *Exponential Phase or Logarithmic (Log) Phase*: The cells multiply at the maximum rate in this exponential phase, i.e. there is linear relationship between logarithm of the number of cells and time. Mass increases in an exponential manner. This continues until one of two things happens: either one or more nutrients in the medium become exhausted, or toxic metabolic products accumulate and inhibit growth. Nutrient oxygen becomes limited for aerobic organisms.

3. *Maximal Stationary Phase*: Due to exhaustion of nutrients or accumulation of toxic products death of bacteria starts and the growth ceases completely. The overall number remains stationary due to balance between multiplication and death rates. Production of exotoxins, antibiotics, metachromatic granules, and spore formation takes place in this phase.

4. *Decline phase or death phase*: In this phase there is progressive death of cells. However, some living bacteria use the breakdown products of dead bacteria as nutrient and re-

main as persister.

Generation times for some common bacteria under optimal conditions of growth are listed below.

Bacterium	Medium	Generation Time (minutes)
Escherichia coli	Glucose-salts	17
Bacillus megaterium	Sucrose-salts	25
Streptococcus lactis	Milk	26
Pseudomonas	Lactose broth	48
Lactobacillus acidophilus	Milk	65-90
Rhizobium japonicum	Mannitol-salts-yeast extract	345-460

3.5 Motility behavior of Bacteria

Bacteria are the simplest free-living single-cell organisms. Bacterial motility is paramount for performing biological functions. Most bacteria possess thin filaments called flagella, which are rigid, helical in shape and are driven by molecular motors at their base [63]. The flagella of the bacteria were imaged by Christian Ehrenberg in *Chromatium Okenii cells* [49]. Advancements in dark-field microscopy carried out by Karl Reichert permitted visualization of flagella bundles in swimming cells, however individual flagella filaments were not resolvable at that time [49, 64]. Subsequently, Thedor Engelmann demonstrated that bacteria do not swim randomly, but respond to chemical stimuli in the surrounding environment. Engelmann demonstrated that an aerobic bacterium concentrates around the regions of high oxygen concentration [57].

Rotation of these flagella produces thrust which pushes cells forward. Bacterial strains may differ in flagella size, function and number. The bacterial motor can change direction of rotation to add additional features to its motility. For single polar flagellated bacteria, such as *P. aeruginosa* and *Vibrio alginolyticus*, the reversing of the motor merely takes it backward. In the case of multiple flagellated bacteria, such as *E. coli*, the co-rotation of multiple flagella filaments often leads to the formation of a single helical propulsive coil referred to as a bundle, the rotation of the helical shaped bundle is sufficient to generate propulsion [65–67].

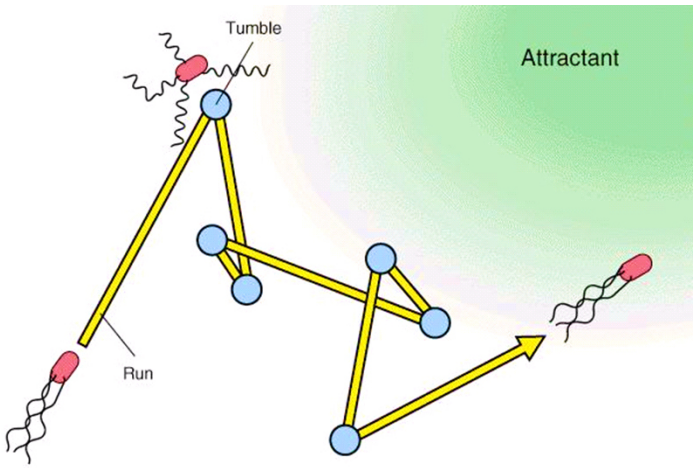

Fig. 3.10 A schematic diagram showing run and tumbling swimming mode.The combination of run and tumble results in a random walk. *Image source geneexp.com*

The thrust generated by the bundle is transmitted along the main axis of the cell body, this maximizes swimming efficiency and minimizes viscous drag. The formation of bundles occurs at one pole of the cell, in the opposing direction of the net motion, helping to direct the cell. The flagella bundle can form at either end of the cell, the swimming efficiency and velocity is intrinsically indistinguishable between bundles formed at either end [57]. When all flagella helical filaments rotate counter-clockwise **(CCW)** they form a flagella bundle, that drives the cell in a forward direction with typical velocities ranging between 20-40μms^{-1} (the average swimming speed of *E. coli* is 25 μms^{-1} [68, 69] and *P. aeruginosa* is 35 μms^{-1} [70, 71]). **CCW** rotation generates relatively straight line swimming trajectories and is recognized as a *run* (as shown in figure 3.10), which lasts for nearly 10 sec. Conversely, when one or more flagella abruptly switches from **CCW** to clockwise rotation **(CW)**, the flagella bundle disperses, thus the swimming stops and the cell body re-orientates randomly because of thermal fluctuations. This process of re-orientation of the cell body is known as *tumble*. It results in varying the swimming trajectory and reducing the swimming velocity (see figure 3.10), and it lasts for nearly 1-2 secs. The initiation of the tumble events occur when at least one or more flagella motors change their rotation direction from **CCW** to **CW**, such that a single filament detaches itself from the bundle, terminating forward motion and casually re-orientating the cell [34]. The change in motors

rotational direction from **CCW** to **CW** induces hydrodynamic stress and load on the flagellum, thus polymorphic transition occurs [34]. Polymorphic transitions change the shape of the flagellum, resulting in random re-orientation often triggered by environmental changes.

The other modes of motility behavior executed by bacteria are: swarming, twitching, gliding and sliding as shown in figure 3.11.

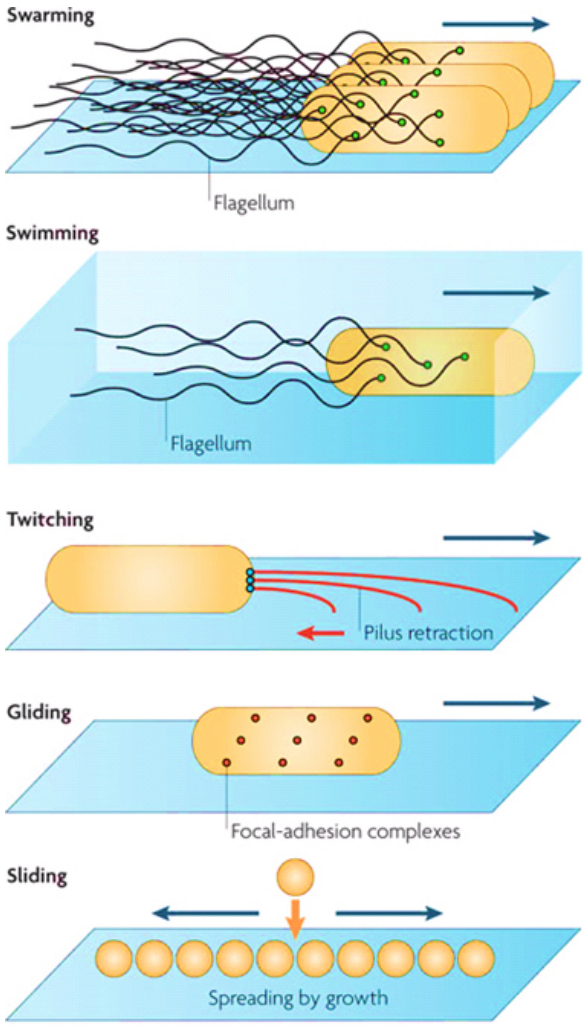

Fig. 3.11 A schematic diagram showing the different modes of motility [34].

Swarming motility is operationally defined as a rapid multicellular movement of bacteria across a surface powered by the rotating flagella. Swarming also requires an increase in flagella number and intracellular interactions. Swimming motility is a mode of bacterial movement powered by rotating flagella but, unlike swarming motility, takes place as indi-

vidual cells, the cells move individually and at random in the same manner as flagellated bacteria move in wet mounts (i.e., nearly straight runs separated by brief tumbling). Twitching motility is surface motility powered by the extension and retraction of pili that confers slow cell movement often with a jerky or twitchy appearance. Gliding motility is a catch-all definition for active surface movement that occurs along the long axis of the cell without the aid of either flagella or pilli. Sliding motility is a passive form of surface spreading that does not require an active motor but instead relies on surfactants to reduce surface tension enabling the colony to spread away from the origin driven by the outward pressure of cell growth. Bacteria such as *P. aeruginosa*, *Vibrio parahaemolyticus* and *Aeromonas* are known for executing swarming behaviors [72].

3.6 Chemotaxis

Bacteria do not always move aimlessly but are attracted by nutrients such as sugars and amino acids and are repelled by many harmful substances and bacterial waste products. Movement towards chemical attractants and away from repellents is known as chemotaxis. Bacteria can also respond to other environment clues such as temperature (thermotaxis), light (phototaxis) and oxygen (aerotaxis).

Among other functions possessed by bacteria, chemotaxis is one of the most studied and well understood phenomena. Cells are able to perform a random walk in order to search for nutrients. Sensors on the cell body enable the detection of chemical gradients directing flagellar rotation accordingly. If a positive gradient is detected, cells tend to continue forward motion, on the other hand, if no gradient or a positive gradient of a toxin is detected , swimming direction is randomized. Repeated application of this sequence helps the cells to perform a three dimensional random walk to look for favorable regions [69, 73, 74].

There have been extensive studies of chemotaxis in *E. coli* cells investigating the intracellular systems for receptor signalling and signalling transduction. Motile *E. coli* actively seek out environments which are deemed to be more beneficial via detecting extracellular chemical signals. Detection of chemical signals is performed by chemoreceptors located at

the poles of the cell, and beneath the cellular membrane. These chemoreceptors are known as methylaccepting chemotaxis proteins MCP's (there are 5 MCP proteins) present in both *E. coli*. Activation of these proteins mediates a phosphorylation and dephosphorylation cascade which switches rotational direction of the motor, i.e. CCW to CW and vice versa to vary the swimming mode from run to tumble. MCPs continuously sample and monitor chemical compounds in the surrounding vicinity, typically every 1 - 3 sec. In response, cells vary their swimming mode, to benefit the cells living conditions. In the presence of chemical gradients such as attractants, the frequency of tumble event is reduced and the average run length of cells are extended in the direction towards the attractant. This bias enables cells to swim towards chemical attractants and away from repellents [69].

Chapter 4

Modeling the Collective Behavior of Active Matter

The term active matter refers to systems whose elementary constituents convert their internal energy into mobility. For this reason they constitute non equilibrium systems. This gives rise to interesting and generally still not completely understood collective motion (as mentioned in chapter 2). Systems made up of microscopic constituents, both living and non-living, have been particularly subjected to theoretical investigation and experimental analysis [75, 76]. In order to provide some insights on the origin of these collective phenomena in 1995 Vicsek$'$s introduced a simple model using the statistical physics approach [77, 78], which immediately found large success and stimulated a lot of further studies.

This chapter gives a brief introduction to Vicsek$'$s model along with flocking behavior which are used to describe the collective motion of microscopic as well as macroscopic active matter. Furthermore it provides the description of our coarse grained model for anisotropic self propelled particles. This model has been developed by Prof. Enzo Orlandini (Department of Physics-University of Padova) and coworkers, it takes into account the excluded volume interaction and the anisotropy of the particles.

4.1 Vicsek′s Model

Vicsek′s model [77] is one of the simplest model to study collective motion. It is the first model which shows the emergence of a dynamic phase transition from a disordered state (in which particles move in random directions) to an ordered state (where they head in approximately the same direction) as the noise level is decreased or mean density is increased. Later models are based on the same approach and are hence extensions and improvements of the Vicsek′s model [79, 80].

The model is characterized by two fundamental features, firstly, the velocity vector of each particle is forced to align with an angular tolerance to the average velocity taken over the neighbors, as a consequence of the interactions. Secondly, the velocity of all particles are set equal to a constant (v_0), modeling the tendency of the units to move at the same speed. The fixed velocity (v_0) provides the out-of-equilibrium character of the system. In fact in the absence of activity, v_0 turns to zero and the model describes simply a set of interacting diffusing particles. So in spite of focusing on how the activity affects the dynamic of the single particle, this model is specifically apt to study the emergence of the coherent motion of the whole system.

The dynamical equations, of the model are given by:

$$\begin{aligned} \mathbf{r}_i(t+\Delta t) &= \mathbf{r}_i(t) + \mathbf{v}_i(t)\Delta t \\ \theta_i(t+\Delta t) &= \langle \theta(t) \rangle_r + \Delta\theta \end{aligned} \tag{4.1}$$

where $\mathbf{v}_i$ is the velocity of the i^{th} particle, $\langle \theta(t) \rangle_r$ denotes the average direction of the velocities of particles (inculding particle i) within a circle of radius r around $\mathbf{r}_i$. The noise term $\Delta\theta$ is a random number chosen with a uniform probability from the interval $[-\eta/2, \eta/2]$, where η is the random perturbation/noise of the system. In general the noise sources can be divided into two groups, i.e. extrinsic noise (*vectorial*) and intrinsic noise (*scalar*). The former noise is due to random perturbation of the individual particle velocity, i.e. the particles do not recognize very well the moving direction of their neighbors. Since it might have to do with the uncertainties in the particle-particle "communication" mechanism therefore

it is termed as the extrinsic noise. The later noise arises from the random perturbation of the average direction of the particle. It is identified as intrinsic because it has to do with internal decision making mechanism of the particle. Here particle can recognize the motion and moving direction of their neighbors but they do not follow them (they "decide" to move in different direction).

A transition from the disordered to the ordered state is found by attuning the agent density and noise amplitude, as shown in figure 4.1. In a disordered state, the system has a random distribution of particle positions and no preferred velocity direction. In the ordered phase, all the particles tend to move in a coordinated direction and aggregate although there is no attractive potential. The order parameter refers to the degree of symmetry that char-

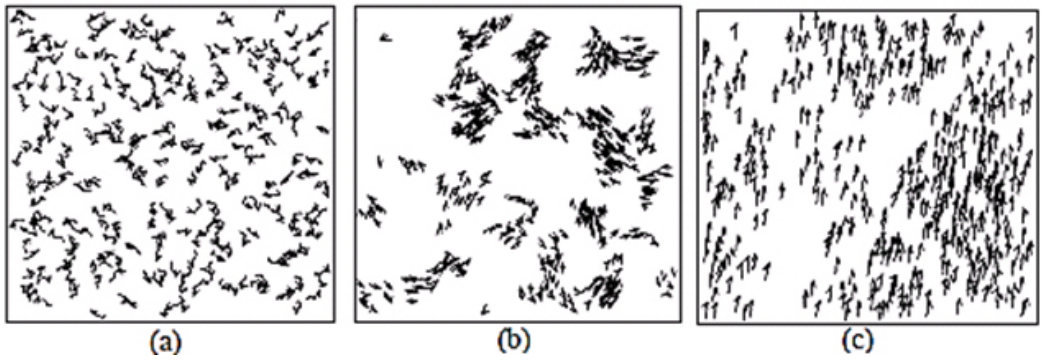

Fig. 4.1 (a) Disordered state with large noise and small density; (b) For small densities and noise the particles tend to form groups moving coherently in random directions; (c) For high density and small noise, the motion of particles becomes ordered [77].

acterizes a phase. Mathematically, this value is usually zero in the disordered phase and non-zero in the ordered phase. However, the nature of the phase transition can depend strongly on the way in which noise is introduced into the system [81]. In order to monitor the collective motion, a suitable order parameter is the normalized average velocity (v_a)

$$v_a \equiv \frac{1}{Nv_o}|\sum_{i=1}^{N}\overrightarrow{v_i}| \tag{4.2}$$

where N is the total number of particles and v_0 is the average absolute velocity and $\overrightarrow{v_i}$ velocity of the i^{th} particle. If the motion is disordered, the velocities of the individual particles point in random directions and average out to give a zero magnitude vector, whereas, for

ordered motion, the velocities all add up to a vector close to Nv_0 (thus the order parameter for large N can vary from about zero to about 1). Hence the Vicsek′s model displays a phase transition from disordered to an ordered state as the level of noise is decreased (see figure 4.2). The Vicsek′s model works nicely in 2D but it requires more numerical effort

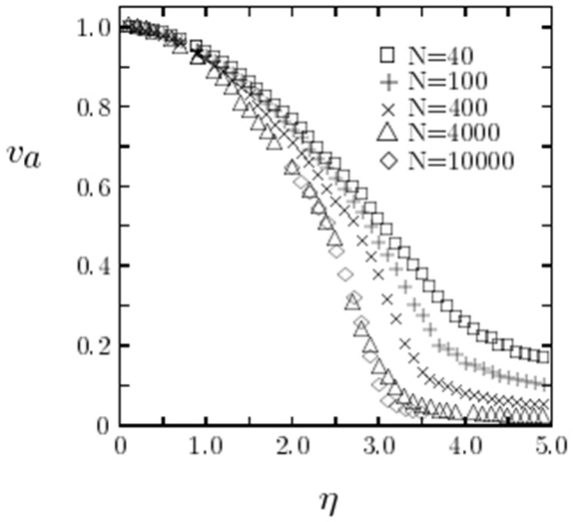

Fig. 4.2 The absolute value of average velocity (v_a) versus noise (η) in particles of various sizes for a fixed density [77].

to accumulate it in 3D where particles have more degrees of freedom and a more complex behavior. In particular the cluster configuration described in terms of cluster size, cluster weight, density fluctuation, cluster speed and cluster life time will be different in 3D. There are other models which describe the behavior of self-propelled particles in 3D space, for instance finite size scaling model by Baglietto et al. [82], slender-body theory by Saintillan et al. [83].

4.2 Flocking Behavior

Models stated in the above section are well suited for microscopic active matter. Instead, dealing with macroscopic living particles the situation changes markedly. In contrast to this, particles mutually interact by means of complex senses (e.g. vision) and their movements are a result of decision making process. The sources of noise that affect the system are

different and mostly unknown, being both internal and environmental. A physical approach cannot aim to fully characterize a given system but rather, targets at identifying the minimal ingredients indispensable to collective motion, and the common patterns (or phases) they give rise to. In this context, flocking is defined as the phenomenon in which macroscopic self-propelled biological particles, using only limited environmental information, organize into an ordered motion [84]. Flocks exhibit strong spatial coherence and are capable of very fast, highly synchronized maneuvers, either spontaneously, or as a response to external stimuli, such as predator attacks or turbulence. In the remarkable work by Ballerini et al. [22], they discovered that each bird interacts on average with a fixed number of neighbors (6 to 7), rather than with all neighbors. They characterized the structure of the flock by the spatial distribution of the nearest neighbors of each bird. Figure 4.3 shows the positions of the individual birds.

Given a reference bird, Ballerini et al. [22] measured the angular orientation of its nearest neighbor with respect to the flock's direction of motion, and repeated this process for all individuals within a flock as reference bird. Figure 4.4 shows the schematic representation of their model, i.e. average angular position of the nearest neighbors.

4.3 A coarse grained model for anisotropic self propelled (microscopic) particles

The Vicsek$'$s model explained in the previous section does not consider the excluded volume interactions between particles and consequently anisotropy of the particles. To have a better comparison with the experimental results, it would be very interesting to see how the statistics is affected by the introduction of these features. To our purpose a new coarse grained model was developed for anisotropic self-propelled particle in 3D. In particular, the model provides a study of collective behavior of self-propelled particles with excluded volume interactions when confined in slit like geometries [2]. This description allows to focus on the importance of steric interactions and activity in determining the density profile of the suspension across the confining region.

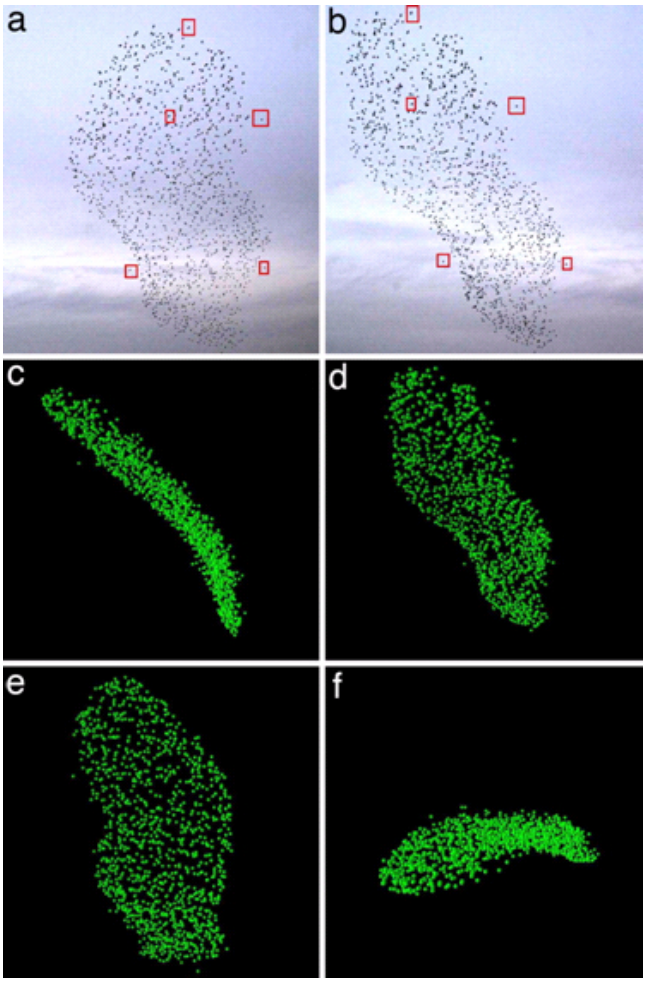

Fig. 4.3 A typical starling flock and its 3D reconstruction. (a) and (b) is the photograph of one of the analyzed flocks. The pictures were made at the same moment by two different cameras, 25 meters apart. For reconstructing the flocks in 3D, each birds image on the left had to be matched to its corresponding images on the right. The small red squares indicate five of these matched pairs. (c-f), the 3D reconstructions of the analyzed flock from four different perspectives. (d) the reconstructed flock from the same view point as (b) [22].

In this model each self-propelled particle is designed as an anisotropic rigid body interacting with one another by excluded volume interaction. Fluid-mediated interactions between particles have been neglected. Computer simulations were performed on systems similar to the experimental ones i.e. suspensions of N_a self-propelled particles containing N_c passive colloidal (ideal) particles. The random effects of the environment on the dynamics is taken into account through a standard Langevin equation.

The model, in sync with our experiment, comprises both self propelled particles as well

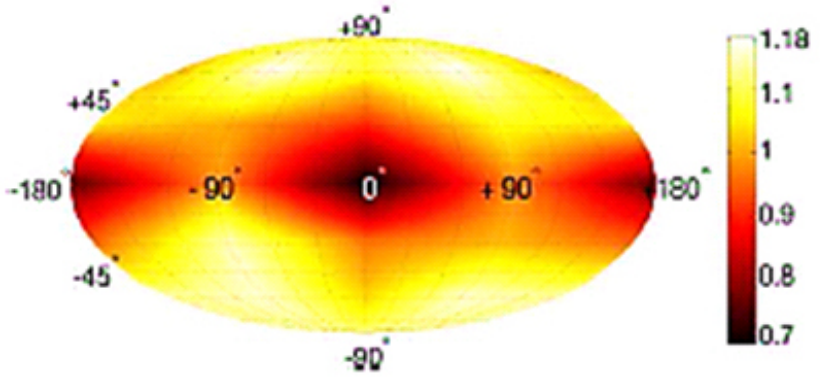

Fig. 4.4 The average angular density of the birds nearest neighbors [22].

as passive colloids, where former represent the motile bacteria and latter represent the non motile one. A self-propelled particle is modeled as a rigid trimer i.e. a body made of three beads, each having a diameter of σ. This gives an anisotropic body of aspect ratio 3. A colloidal passive particle is described instead as a single bead of diameter σ_c=2σ. Each bead of diameter σ interacts with the other 3(N_a-1) by means of a truncated and shifted Lennard-Jones potential given as:

$$V_{i,j}^{L,J}(r) = \{4\varepsilon\left[\left(\frac{\sigma}{r}\right)^{12} - \left(\frac{\sigma}{r}\right)^{6} + \frac{1}{4}\right]\}\theta(r - r_c) \tag{4.3}$$

where r=$r_i - r_j$, with i, j=1,2.....3N_a (N_a is the number of anisotropic self-propelled particles), r_c= $2^{1/6}\sigma$, ε sets the strength of the interaction and θ is the Heaviside function. The hard sphere colloids interacts with other constituents (trimers and colloids) via the same truncated and shifted Lennard Jones potential where now σ in (equation 4.3) is half the sum of the hard core diameter of the two interacting beads (either belonging to a trimer or colloidal particle). Self propulsion in the trimers is introduced by a force $\overrightarrow{F}_a$ acting on each bead such that the force acting on each trimer has modulus 3$|\overrightarrow{F}_a|$ and the direction given by the trimer "director" pointing, along the major axis of the trimer, from the rear bead to the front one (head). For each trimer its head is chosen randomly at the beginning of each simulation. Finally the system is sandwiched between two impenetrable walls at Z=0 and

Z=L_z as shown in the figure 4.5. Along the x and y directions periodic boundary conditions (with periodicity L_x and L_y) are considered. The time evolution of the trimers is obtained

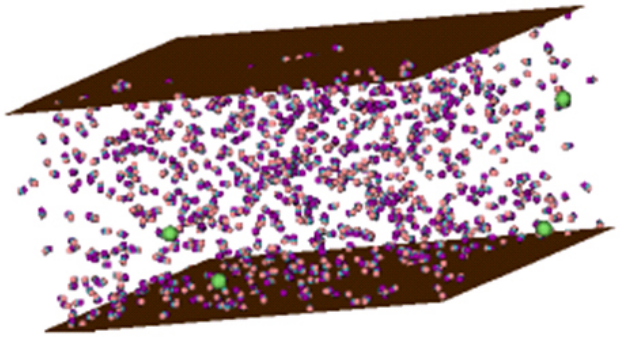

Fig. 4.5 Suspension of self propelled trimers and colloidal particles (in green) between the two walls.

by integrating numerically, using the LAMMPS (Large-scale molecular massively parallel simulator) molecular dynamics package, the coupled Langevin equation of motion for rigid bodies of 3 beads. Each simulation is started from an initial configuration where trimers center of mass positions and orientations are randomly chosen (with uniform probability) while velocities come from a random uniform distribution at a given temperature (room temperature in our case). Figure 4.6 shows simulation studies of the density profile of bacteria across the slit (for the slit width ($L_z = 70\mu m$) at different average volume fraction. The volume fraction is given as:

$$\phi = \frac{3N_a\frac{4}{3}\pi(\frac{\sigma}{2})^3}{L_xL_yL_z} = \left(\frac{\pi}{2}\frac{N_a}{L_xL_yL_z}\right)\sigma^3$$

An important aggregation near either wall is observed. The effect of aggregation near the walls does not depend qualitatively on the average concentration and it quantitatively comparable with the experimental data.

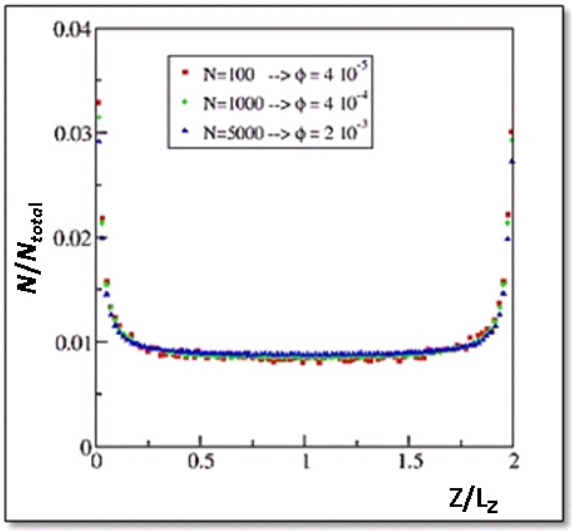

Fig. 4.6 Simulated concentration profile of swimmers as a function of the normalized distance between the two walls of the slit (the walls distance is $70\mu m$). Different symbols refer to different values of swimmers occupation volume ϕ.

To show that the degree of accumulation at the wall depends on the amount of activity of the swimmers Orlandini et al. simulated the system as described above with different Peclet number[1]. At fixed temperature this corresponds to consider different level of activity of the swimmers. Figure 4.7 shows the concentration profile across the slit for swimmers with different P_e (different symbols corresponds to different activity). As expected, as the activity decreases the condensation at the walls weakens. Orlandini et al. also carried out simulation study to show the density profile for different values of slit width. It is evident from figure 4.8 that for fixed volume fraction (ϕ), density distribution pattern varied with a variation in the confinement size. They found that as the confinement size is reduced, the aggregation level enhanced but there is a quantitative enhancement of the density at the proximity of the walls, irrespective of the confinement size, for all the slit widths used in

[1]Péclet number (P_e) is one of the important parameter in describing bacterial motility. It is defined as the ratio of the diffusion time and advection time $P_e = \frac{T_D}{T_v}$ where $T_v \sim \frac{L}{V}$ and $T_D \sim \frac{L^2}{D}$ which can be interpreted as the time required for a particle with a diffusion coefficient D to move a distance L. This gives

$$P_e \sim \frac{VL}{D}$$

where V is the characteristic velocity and L is the characteristic length of the bacteria

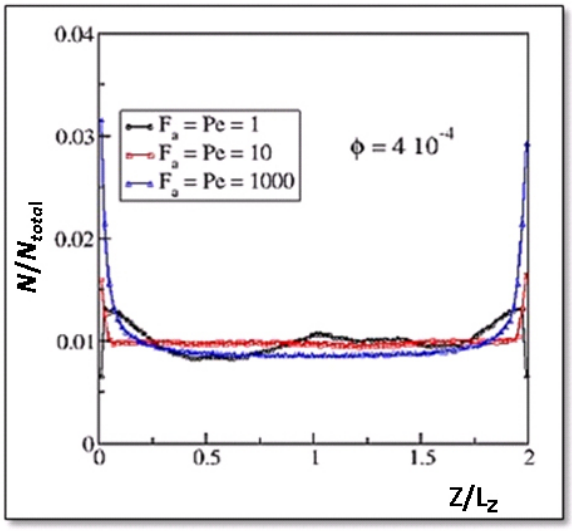

Fig. 4.7 Simulated concentration profile of swimmers as a function of the normalized distance between the two walls of the slit (with the slit width of 70 μm), while $L_x = L_y = 200\sigma$. Different symbols refer to different values of the activity (i.e. different values of P_e) of the swimmers.

the simulation.

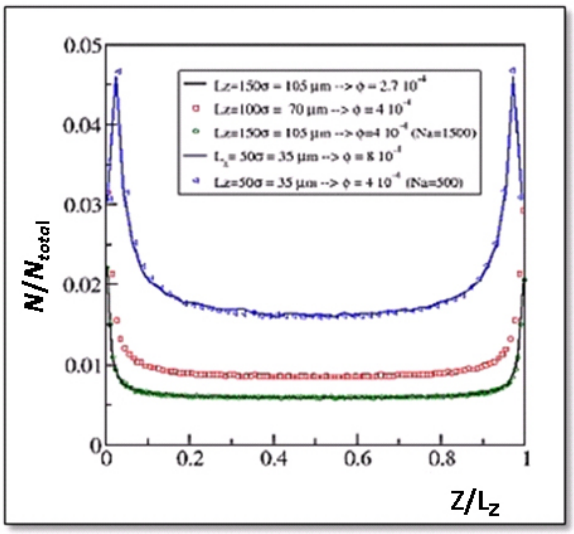

Fig. 4.8 Simulated concentration profile of swimmers as a function of the normalized slit width. Symbols refer to systems having the same volume fraction confined in slits with $w = 35, 70, 105\mu$.

Thus, Orlandini et al. simulation result also shows the density enhancement of bacteria near the walls which is similar to the one shown in the original work by Breke et.al [2] but with a different approach. The model suggests that steric interactions and activity (propul-

sion)are the physical parameters affecting the spatial distribution of bacteria. Due to these interactions, these rod shape particles get aligned parallel along the surface of the walls leading to density enhancement. A comparison of our experimental result with simulation has been shown in chapter 6.

Chapter 5

Sample Preparation Methods and Characterization Setups

Microbiology is usually concerned with organisms so small they cannot be seen distinctly with the unaided eye. Because of the nature of this discipline, the microscope is of crucial importance. Thus it is important to understand how the microscope works and the way in which samples are prepared for examination. This chapter discusses the standard microbiology techniques and procedures employed in bacterial characterization and synchronization. A brief description on some of the physics of an optical microscope and of the microscopy techniques used in our experiment have been depicted in this clause. This chapter also enumerates the basic techniques used to compute the growth rate of bacteria, together with a brief explanation on sample preparation method and density matching fluid have been also presented here. Finally, it illustrates the tracking software used for image analysis.

5.1 Optical Microscopy

The human eye is nature's evolution of a lens system which allows us the ability of sight. Vision is a sophisticated process by which the eye lens forms an image into the retina by rays entering the pupil [85]. Moreover, the lens system in our eyes can focus by the contractions of the ciliary muscles. This allows the eye to focus on objects which are a few centimeters

to several meters away. However, the human vision has a limited resolution; the smallest objects one can observe with the naked eye are in the order of $\approx 500\mu m$ [86]. To achieve higher magnification, one brings the object closer to the eye. At very short distances the eyes magnification is limited and fine details become "*blurred*" when the object is too close to the eye [87]. A solution to this limitation of the eye is to devise a simple magnifying lens system where a single lens can achieve up to 10 X more magnification, as shown in figure 5.1. Magnification is defined as:

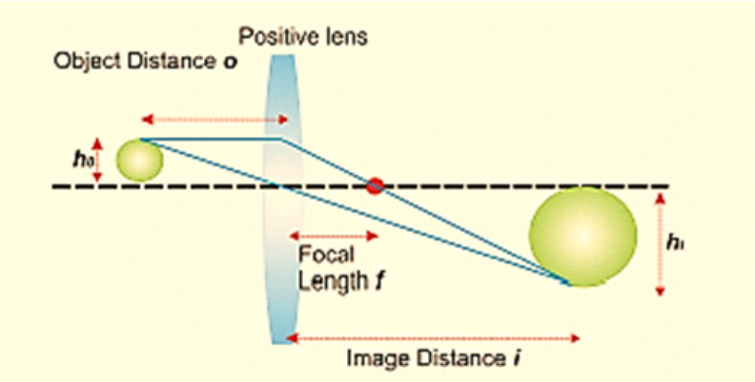

Fig. 5.1 Using a ray diagram to highlight how a simple single lens system is capable of magnifying an object/image with a focal length *f*.

$$M = \frac{h_i}{h_o} \tag{5.1}$$

where h_o and h_i are the height of the original object and the image of the object respectively (see figure 5.1). Objects which appear on the micron range are un-resolvable from a simple magnifying lens. To acquire significant magnification a series of lenses are required, giving rise to an optical microscope. Microscopes provide high magnification of small objects with good resolution which is limited to the sub-micron range. The basic components of a microscope consists of an objective lens, a condenser lens, an illumination source and an eyepiece. These essential components of a microscope are shown in figure 5.2. The objective lens initiates the first stage of the magnification process in the microscope system. The objective lens generates a magnified image of the sample at an infinite distance and the role of the tube lens is to focus the parallel rays of the magnified image onto the intermediate

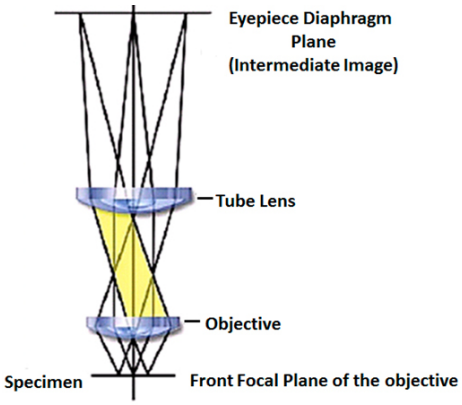

Fig. 5.2 A schematic diagram of a compound microscope. The objective lens images the specimen and is projected onto the intermediate image plane via the objective and tube lens (condenser lens).

image plane of the eyepiece lens depicted in figure 5.2.

There are two types of commonly used microscopes, the up-right microscope as shown in figure 5.3 and the inverted microscope shown in figure 5.4.

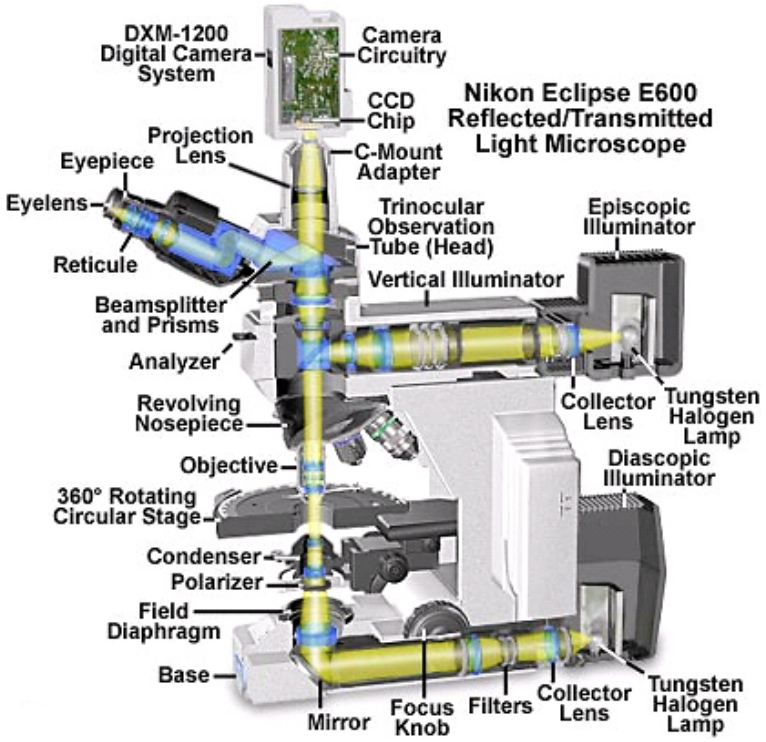

Fig. 5.3 A schematic diagram of light path of a Nikon eclipse. In an up-right microscope the light source emerges from below the sample stage and illuminates the sample from underneath and projected onto the objective lens.

The most commonly used microscopes in the field of microbiology are up-right. They contain a tungsten-halogen lamp which is utilized as an illumination source. The emitted rays are collimated by a collector lens and are directed towards the main optical axis of the microscope located via a mirror at the base. The illumination source propagates through the field diaphragm and is focused by the condenser lens which is focused on the sample. The objective lens magnifies these propagating light rays and projects them onto a beam-splitter, either diverting the image to the eye piece or to a camera port. The up-right microscope houses the sample on the stage which permits accurate positioning and focusing of the samples. The illumination and contrast is controlled by various apertures in the optical path. The upright design focuses the sample via controlling the distance of the stage in relation to the objective lens, thus the stage translates in vertically.

An inverted microscope design is depicted in figure 5.4. The key distinguishing features which separates this design from the up-right design is the optical light path and the location of the objective lens. In an inverted microscope, the illumination source is above the sample stage. Light rays propagate through the field diaphragm and other filters, subsequently being deflected via a prism along the main optical path parallel to the optical axis. The light path is focused by a condenser lens onto the sample; this achieves uniform illumination of the sample. The objective lens is located beneath the stage on a revolving nosepiece pointing upwards onto the main optical axis of the microscope. The magnified image is then projected through the eyepiece or towards a camera port using a series of beam splitters and prisms.

The main advantage of using an inverted microscope rather than a conventional up-right one is that it gives greater access to the sample stage area, permitting physically larger sample to be imaged from below. The inverted microscope is excellent at observing motile bacteria at the bottom of petri-dish, glass-slide or in a container under a more natural environmental condition. The inverted design allows significantly easier access to the condenser lens where additional optical components can be inserted. However one of the limitations of the inverted design requires the bottom interface of the sample to be relatively thin e.g. ≤ 1 mm, because it is often difficult to obtain good imaging with sufficiently thick samples.

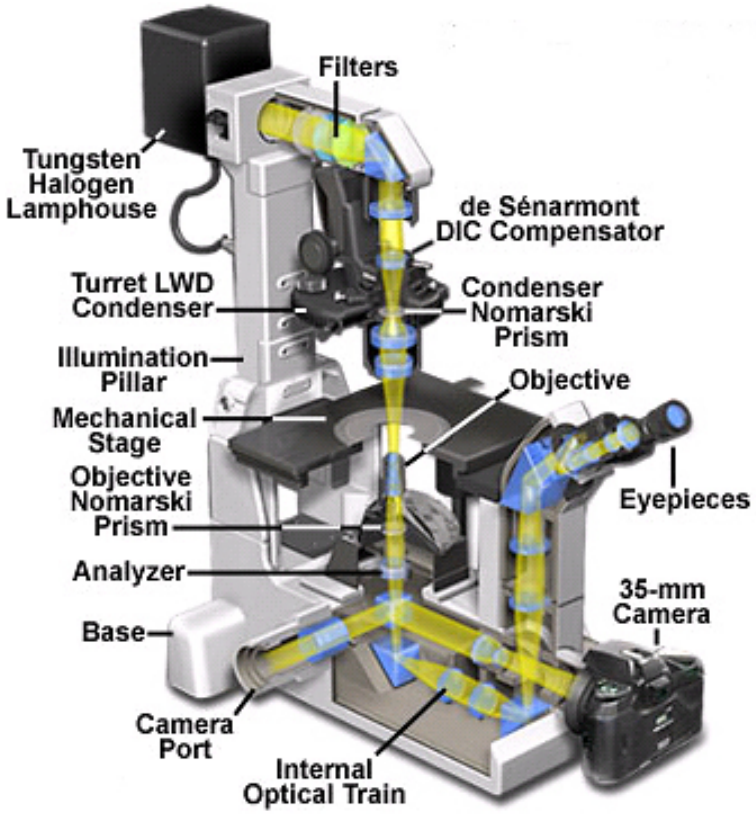

Fig. 5.4 A schematic diagram of an inverted microscope (from Nikon) depicting the optical light path. The illumination source is located above the sample stage along with the condenser lens. Note, the location of the objective lens is below the stage where samples are mounted.

Overall both designs have their advantages depending on their specific applications.

When using a microscope (whether up-right or inverted) the image quality is determined by several factors such as the total magnification, i.e. the magnification of the objective lens, tube lens and eyepiece combined. The more powerful the objective lens, the higher magnification one can acquire; although high objective magnifications $\geq$ 500 X is meaningless if the resolution is not sufficiently high [88, 89]. This effect is referred to as empty magnification since no additional details are achieved with additional high magnification. To distinguish fine details one must *resolve* the image to identify minute features. These tiny features are defined by resolution or resolving power of the microscope.

5.2 Microscope Resolution

The most important part of the microscope is the objective, which must produce a clear image, not just a magnified one. Thus, resolution is extremely important. Resolution is the ability to separate or distinguish between small objects that are close together [85, 90].

Resolution is described mathematically by Abbe equation. It was developed by Ernst Abbe in the year 1870 [91]. Abbe equation states that the minimal distance *(d)* between two objects that reveals them as separate entities depends on the wavelength of light λ used to illuminate the samples and on the numerical aperture (N.A.) of the objective. The relationship is defined as:

$$d = \frac{0.5\lambda}{nsin\theta} \tag{5.2}$$

where $(nsin\theta)$ is N.A. of the lens, n is the refractive index of the medium in which lens work (i.e. oil or water immersion) and θ is half-cone angle of light entering the objective as illustrated in figure 5.5. As d becomes smaller (from equation 5.2), the resolution increases

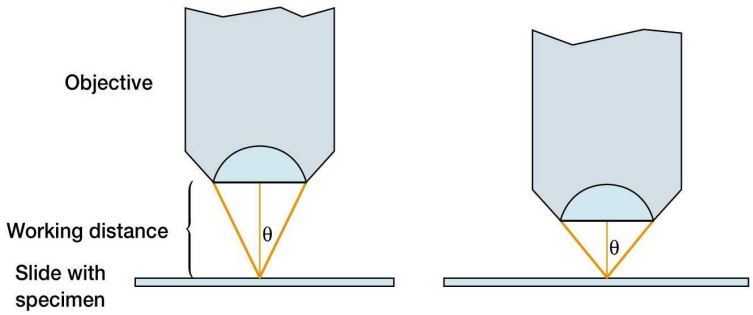

Fig. 5.5 The angular aperture θ is half-cone angle of light that enters a lens from a sample, and the numerical aperture is $nsin\theta$. In the right-hand illustration the lens has larger angular and numerical apertures; hence its resolution is higher.

and finer details can be discerned from the samples. Thus, the greatest resolution is obtained by using a lens with the largest possible N.A. and light of the shortest wavelength. The other contributing factor which determines the resolution is given by light diffraction and refraction, which can be tuned by oil immersion. Figure 5.6, illustrates the improvement in resolution and imaging quality obtained by immersing the objective in a transparent oil

having a suitable index of refraction. Figure 5.6(a) shows an air gap which separates the

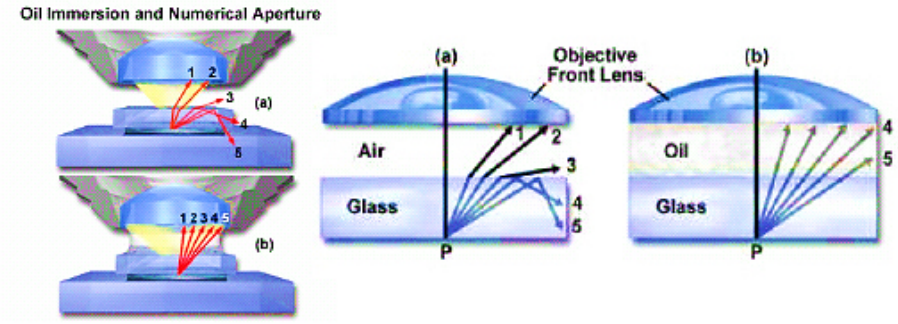

Fig. 5.6 A ray diagram showing the effects of oil immersion on the numerical aperture and resolution. (a) Shows a sample without oil where rays are refracted (b) Shows a sample with oil which eliminates refraction and the majority of the rays are collected by the objective.

samples from the objective lens. The propagating light has to travel through two media, glass and air, where there is sufficient contrast in refractive index n. According to Snell's law, the propagating light beam is deflected, $n_{air} < n_{glass}$ thus the exiting angle is larger (as shown in figure 5.6) [86]. Therefore fewer rays of the propagating light beam are collected by the objective lens. However, by inserting an immersion liquid such as oil or water to refractive index match either the glass slides or the sample itself (see figure 5.6 (b)) the amount of refraction is reduced. This also decreases optical aberrations thus achieving higher numerical aperture, thereby increasing the resolution. Figure 5.7 is the picture of the microscope of our lab, which was used for this research project.

5.3 Optical setup

The image acquisition system consists of a microscope, a CCD camera and a computer with software to control and automate the measurement. A Nikon M450E inverted microscope (Eclipse, Ti-E) composed of a TI-SR rectangular mechanical stage and CFI-10X eyepieces was used for our experiment. The microscope was configured for Bright-field microscopy and a 12V halogen lamp (100W) connected with a power supply was used as the illumination source.

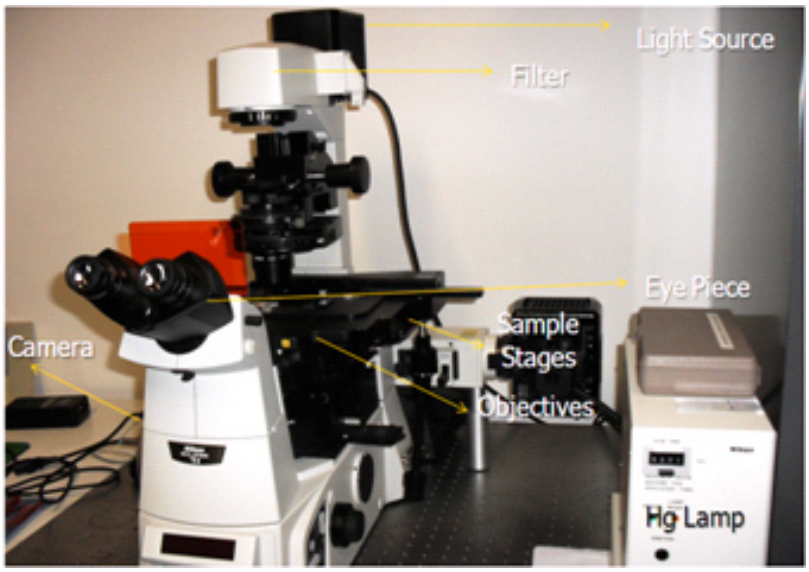

Fig. 5.7 A picture of the Nikon microscope use in our lab for image acquisition.

We used an Andor Luca-S camera with a resolution of 659 X 496 pixels for the image acquisition. The camera has an EMCCD (Electron Multiplying Charge Couple Device) sensor. This sensor is extremely sensitive and capable of detecting up to a single photon under optimal conditions. The sensor of the camera is equipped with a cooling system to bring it to the condition of optimal single-noise ratio. The images we generally acquired at a speed of 32 fps (frame per seconds). The camera is mounted on a Nikon Eclipse Ti-E

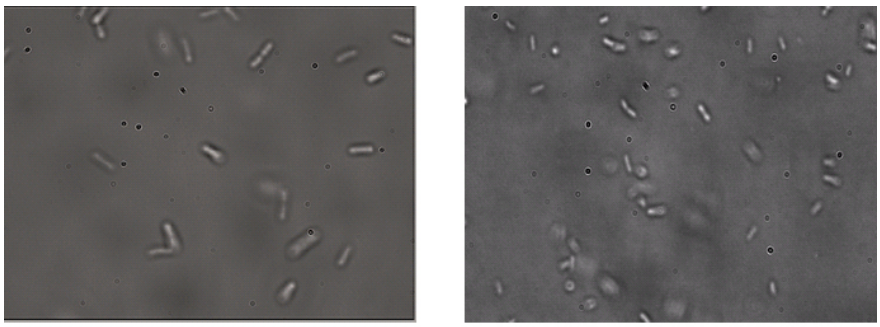

(a) *E.Coli* (b) *Pseudomonas*

Fig. 5.8 A micro-graph showing the images of bacteria taken in our lab (a) *E. coli* and (b) *Pseudomonas*.

inverted microscope as shown in figure 5.7. The objective stage is motorized and the focus

can be controlled either by computer or with a knob attached to the microscope. The motor that moves the lens in the vertical direction (lateral) has a minimum pitch of 0.025 μm and the position can be adjusted manually in coarse, fine or extra-fine mode. The state-of-art is very accurate and stable. The microscope is equipped with numerous accessories, including rings for phase contrast, filters, dichroic lamp for fluorescence and neutral density filters.

An Olympus 100X water immersion objective (with the numerical aperture of 1) was used for image acquisition. It has a good contrast sufficient enough for the tracking software. With this objective bacteria can be easily distinguished (see figure 5.8). Its reduced depth of field (1-2 μm) and high working distance (1.5 mm) are its two main characteristics. The latter feature makes this objective perfect for the experiment because it can cover the entire vertical distance between the two cover-slips and spacer, which is at most of a few hundreds of micron.

The Nikon NIS-Element software was used to capture the image sequences. This acquisition system was fully automatized by writing a small "macro". The scan along the vertical direction (Z-scan) was obtained by moving the focal plane from the bottom wall to the top wall (or vice versa). The images were taken at regular intervals. The scan was carried out by the use of software by setting up the parameters such as initial and final position of the bottom and top wall, step size and exposure time (see figure 5.9).

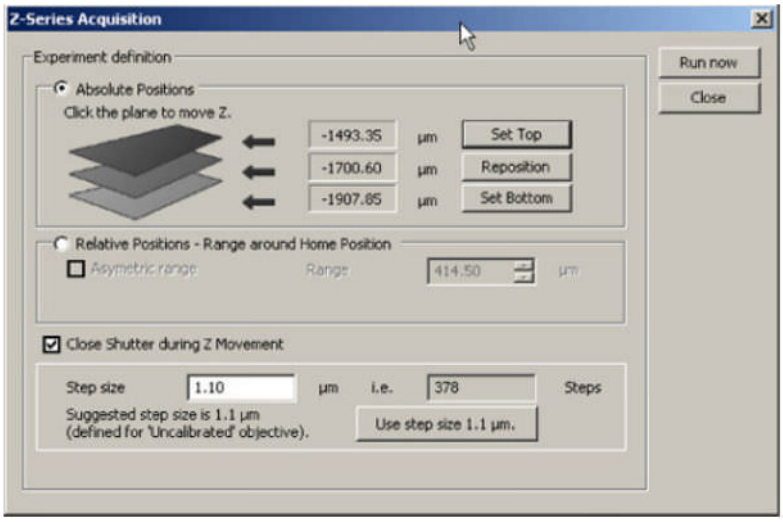

Fig. 5.9 A screen shot of the acquisition software.

5.4 Preparation and characterization of bacterial solutions

5.4.1 Bacterial growth

Motile *Escherichia coli (E. coli)* and *Pseudomonas aeruginosa (P. aeruginosa)* strains were isolated from clinical specimens collected at the Microbiology and Virology section, University Hospital of Padova. Bacterial strains were grown at 37^oC for 16 hours in Luria broth (LB) containing 1.0 % tryptone, 0.5 % yeast extract, and 1.0 % sodium chloride at final pH = 7.0. Culture was then diluted 1:300 in fresh medium and grown at 37^oC until an optical density equal to 0.375 at 600nm was reached, corresponding to mid-log phase of growth. Bacterial cells were then harvested by centrifugation (2,200 rpm for 10 minutes) and washed twice to ensure growth medium depletion. Bacteria were finally resuspended in pre-warmed fresh LB.

5.4.2 Measurement of density of bacterial population

Direct microscopic count

The direct microscopic count is an easy, simple and relatively rapid method to enumerate bacterial cells in liquid medium. The method requires minimum equipment, using a microscope and special glass slides known as counting chamber, consisting of a ruled slide and a cover slip [92, 93]. Different counting chambers are available in the market, each one characterized by the depth and size of the ruler (grid). In this study, the Petroff-Hausser counting chamber was used to determine bacterial concentration. This special designed counting chamber is characterized by a grid system etched on the bottom of the chamber as depicted in figure 5.10. The area of the square of the grid is 2500 μm^2; the depth of the chamber is 10 μm. The space beneath the slide and the cover slip was filled with 100 μl of bacterial suspension prepared as described in 5.4.1 and directly visualized at the microscope. The number of bacterial cells in three different squares of the grid was counted. The average number of the cells was calculated and the density of bacteria in the original culture

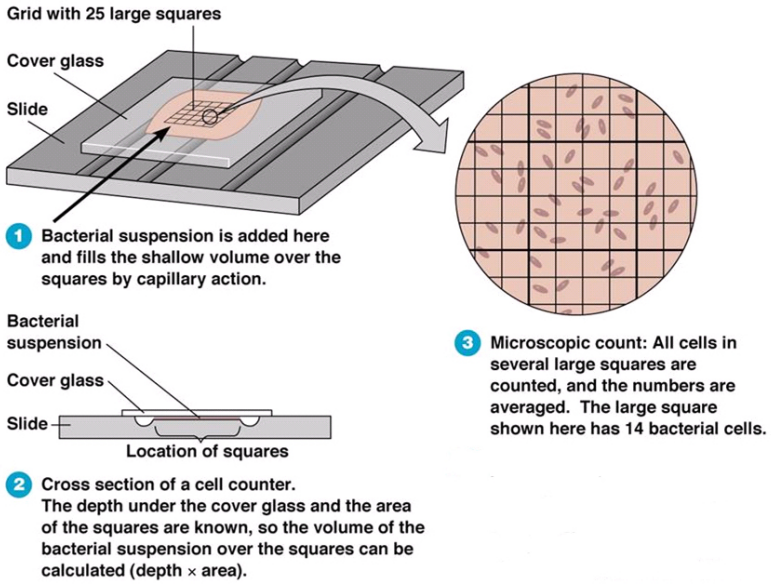

Fig. 5.10 A schematic of Petroff-Hausser Counting Chamber.

was determined by extrapolation:

$$n = \frac{N_T}{A\,(\mu m^2)\,\cdot\,D\,(\mu m)} \tag{5.3}$$

where n is the density of bacteria, N_T is the total number of bacteria counted in a square, A is surface area of the square and D is the depth of the counting chamber. Figure 5.11, shows the counting chamber with and without bacterial suspension. The major advantage of the

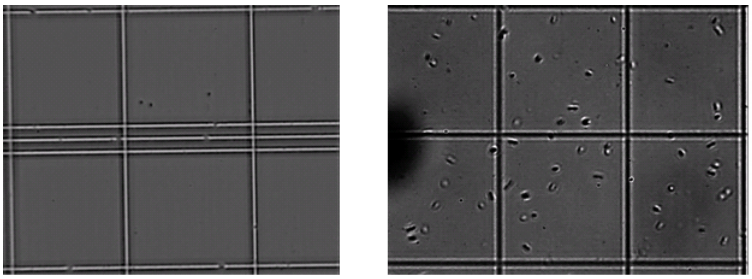

(a) Counting Chamber (without cell suspension)

(b) Counting Chamber (with cell suspension of *Pseudomonas*)

Fig. 5.11 Image of counting chamber taken during the experiment.

direct microscopic count is the speed at which results are obtained. However, by using this

method it is not possible to distinguish living from dead cells. Moreover, accuracy of the counting is not reliable as only a small volume of the original bacterial culture is sampled. Finally, motile bacterial cells are very difficult to count, resulting in wrong estimation of bacterial density. Thus, the direct microscopic count method is not very useful for determining the number of viable motile bacterial cells.
For these reasons we moved to determine the density of bacterial suspension by using indirect methods.

Standard plate count

Bacterial suspensions prepared as described in 5.4.1 were used to set up serial 1:10 dilutions. Briefly, 1 mL of bacterial suspension was transferred into a new tube containing 9 mL fresh LB as depicted in figure 5.12. Then, 0.1 mL of each dilution was transferred to LB agar plates (which is LB containing 1.0 % Bacto agar) and spread. LB agar plates were then incubated at $37C^o$ for 16 hours. During incubation, each bacterial cell (unit) grew and formed one bacterial colony (figure 5.13). The density of the original sample is determined by counting the colony-forming units (CFU) and correcting the results by the dilution factor. To rule out experimental bias and random error, we performed the experiments in duplicate. Thus, at the same time two technical repetitions for 1:10 dilutions and for the subsequent spreading of culture on agar plates were carried on. The final counting of CFU was then compared to validate the reproducibility of the results. Enumeration of colony-forming units (CFU) is a valid technique to estimate living bacteria in the initial suspension. However, since this technique is time-consuming and requires more than 16 hours, it is not routinely used in microbiological experiments to evaluate the density of bacterial suspensions. For these reason, calibration curves are usually set up by coupling the standard plate count technique with the turbidimetric measurement of the bacterial suspension [94].

Turbidimetric measurement

Turbidimetry is the measurement of light-scattering species in solution. It is evaluated by the decrease in intensity of incident beam after it has passed through the solution. Thus,

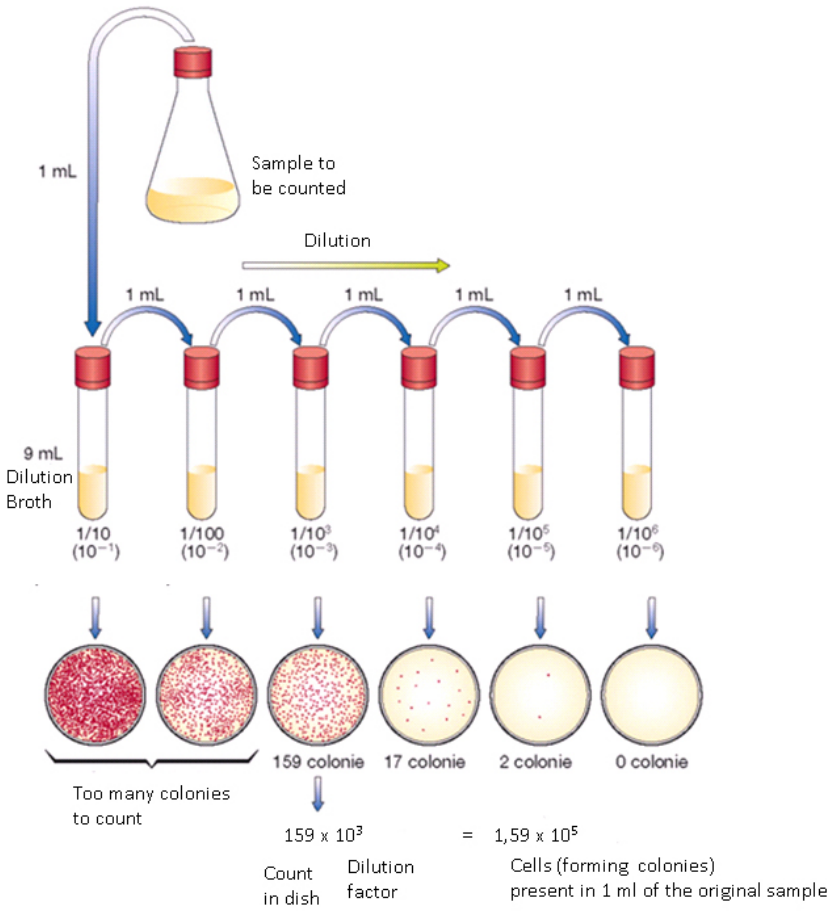

Fig. 5.12 A schematic diagram to illustrate the method for series of dilutions ranging from 10^{-1} to 10^{-6}. Each plate is incubated for 16 hours at $37C^o$, the plates depicts a depleting number of colonies grown in each dilution.

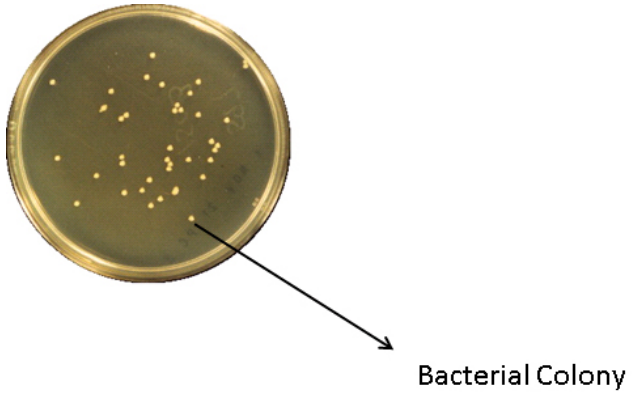

Fig. 5.13 A plate depicts a depleting number of bacterial colonies.

increase in light adsorbance (i.e. the total light-blocking power of a certain suspension with a defined thickness) is directly proportional to the augment in the density of the solution [95, 96]. The extent of light adsorption can be evaluated by using a spectrophotometer set at the wavelength 600 nm (see figure 5.14).

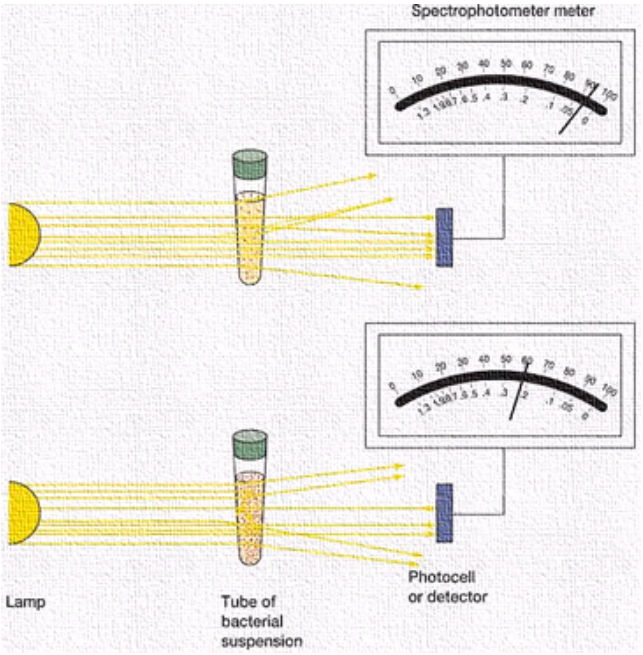

Fig. 5.14 A schematic representation of optical spectrophotometer set-up.

In spectroscopy, the adsorbance measurement (A) is calculated using the following relation:

$$A = -log\ T = -log\ (I/I_0) \tag{5.4}$$

where T is the light transmitted through the sample, I is the light intensity after it passes through the sample and I_0 is the initial light intensity [97, 98].

Thus, final OD is defined as:

$$OD = \frac{A}{L} \tag{5.5}$$

where, L denotes thickness of sample holder.

In our experiments, the density of bacterial suspensions prepared as described in 5.4.1

and diluted 1:10 as described for the standard plate count were evaluated with a spectrophotometer. The OD values were then plotted against the number of CFU enumerated in the same bacterial suspensions grown on LB agar plate to set a calibration as depicted in table 5.1.

OD	CFU
0.14	112000000
0.1	80000000
0.091	72800000
0.085	68000000
0.078	62400000
0.067	53600000
0.042	33600000

Table 5.1 Calibration values prepared using the optical density measurement and the plate counting (CFU) technique.

Independent experiments performed in our laboratories demonstrated that the OD values recorded in *E. coli* and *P. aeruginosa* cultures grown under constant conditions reported reproducible number of CFU, thus validating the use of the turbidimetric method for a rapid evaluation of the density of motile, living bacterial cells.

Figure 5.15 represents the plot of OD versus CFU. Therefore, to determine the concentration of a solution of *E. coli* or *P. aeruginosa*, we first have to perform the OD measurement and the final density can be estimated as, for example if the OD is 0.085, the corresponding formula is:

$$1 : 8 \times 10^8 = 0.085 : X \tag{5.6}$$

With the recent advancement in the field of optics, the measurement of optical density has become a common and more reliable method to quantify various important parameters like

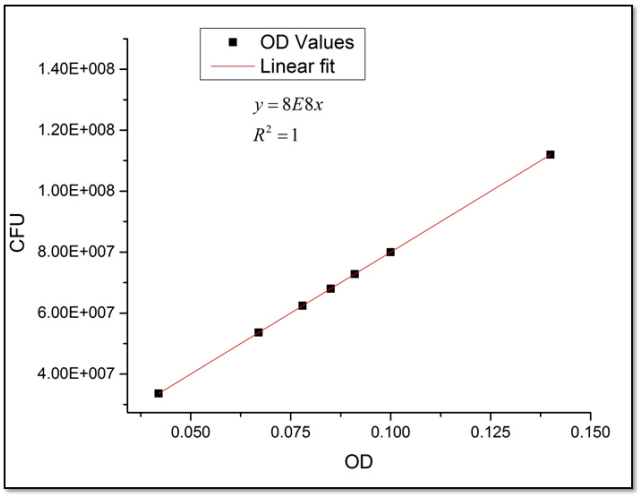

Fig. 5.15 Variation of OD with CFU where dots represent experimentally obtained OD values and solid line represents their linear fit.

concentration of cell, production of biomass or alternation of cell morphology [99].

5.4.3 Preparation of bacterial suspensions for motility assay

Once validated the calibration curve, *E. coli* and *P. aeruginosa* were grown in LB as described in 5.4.1. Density of bacterial population was then evaluated by the turbidimetric method. Based on the calibration curve previously set up, 1.5×10^{-2} CFU/mL were washed by centrifugation and finally resuspended in motility buffer containing KH_2PO_4 10 mM, HEPES 0.1 mM, glucose 0.2 %, pH 8.2 [100]. The final solution of bacteria was mixed with Percoll to match the cell bounancy density. Bacteria were then immediately used for motility studies.

5.5 Percoll

Percoll is considered to be a well-referenced medium for density matching fluid for cells, viruses, and subcellular particles. It was introduced by Prof. Hakon Pertoft in the year 1977, and thereafter has become the choice of thousands of researchers worldwide for density gradient medium. Its non-toxic nature and compatibility with biological materials makes it ideal for microbiological application.

Percoll is a silica sol colloid that can be used as a tool to match the medium and cell buoyant densities [101, 102]. Figure 5.16 shows the electron microscopy view of Percoll particles. Silica particles are composed of a poly-disperse colloid having a size of 15 to 30

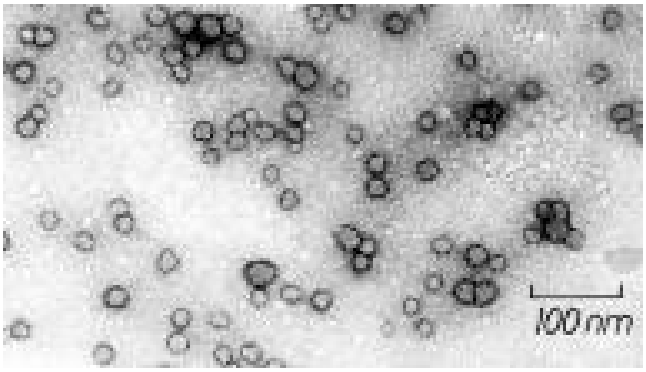

Fig. 5.16 Percoll particles as viewed under Electron Microscope.

nm in size, with a mean particle diameter of 21-22 nm. These silica particles have nondialyzable polyvinylprrolidone (PVP) coating, preventing them from penetrating cell membranes and rendering them non-toxic to cells and sub-cellular particles [103, 104]. Some of the important physical properties of the Percoll particles have been stated in Table 5.2.

Property	**Value**
Density	$1.130 \pm 0.005\ g/ml$
Osmolality	$< 25\ mOs/kg\ H_2O$
Viscosity	$10 \pm 5\ cP\ at\ 20^o\ C$
Conductivity	$1.0\ mS/cm$
pH	$9.0 \pm 0.5\ at\ 20^o\ C$
Refractive index	$1.3540 \pm 0.005\ at\ 20^o\ C$

Table 5.2 A brief summary of the physical properties of the Percoll particles.

The pH of the Percoll solution can be adjusted to 5.5-10.0 by adding buffered solution. No change in properties occurs within that range, allowing Percoll to be adjusted to the optimal growth pH for cells (pH of approximately 7) without altering its effectiveness. Both its physiological pH and its physiological ionic strength help cells stay in a favourable environment during the experiment.

5.6 Tracking Software

This section describes the tracking software which was, used to track and count the cells. The program has been written by Dr.Enrico Chiarello [1] . The software uses the techniques of *"computer vision"*, in particular the one that is used to analyze the images of the bacteria acquired with microscope, from which we can extract the number of motile bacteria. The term computer vision generally refers to a set of techniques that allows the computer to see the objects inside the image and enables us to extract the useful information from them (see figure 5.17) [105, 106]. The tracking software is based on OpenCV, which is a generic

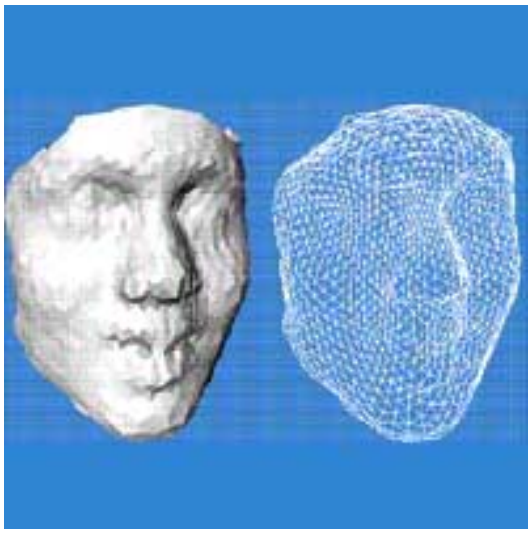

Image source ri.cmu.edu

Fig. 5.17 A 3D view of human face with bit-map information.

library of computer vision. OpenCV has a GPL license, and can be downloaded for free from the internet [107].

The algorithm of the program allows us to perform the following operation. Figure 5.18 shows the work-flow of the software. Following are the sequence of operations performed for the tracking of bacteria:

- Organization of images: All acquired images can be viewed, by varying the parameter (Z-Space); (six hundred images have been taken during the image acquisition for good

[1] lafsi.fisica.unipd.it-2013-Chiarello-attrazione-dinamica-batteri-sup.pdf

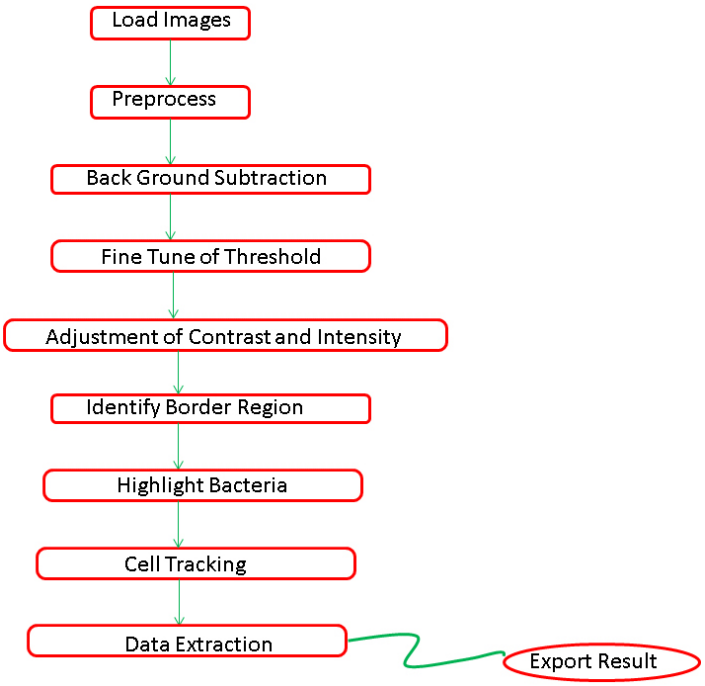

Fig. 5.18 A schematic of cell tracer workflow.

statistics)

- Allows adjustment of the contrast (see figure 5.19b).
- It can implement the operation "top-hat" to highlight the peaks, i.e. for the bacteria, that appear lighter in the background as shown in figure 5.19d.
- The result of the "top-hat" that belongs to the foreground (i.e. that falls below the foreground mask) is applied as threshold (pre-filtering).
- In the due course of the threshold the connected components are labeled as shown in figure 5.19e.
- For each bacteria thus found, a calculated position (centroid), area and the smallest box that contains them are adjusted (figure 5.19f). The number of connected components corresponds to the total count of bacteria i.e. motile and non-motile.
- The tracking is performed for the non-motile bacteria, which are those that have moved very little (just due to Browian motion) from the first sequence of image to

next sequence. Henceforth, a bacterium is counted as "non-motile" if its centroid falls inside the box of previous bacterium. Non-motile bacteria exhibit the same behavior and hence they are given a label or unique number. The operation is repeated for entire sequence of images, finally the bacteria which are different from the label are

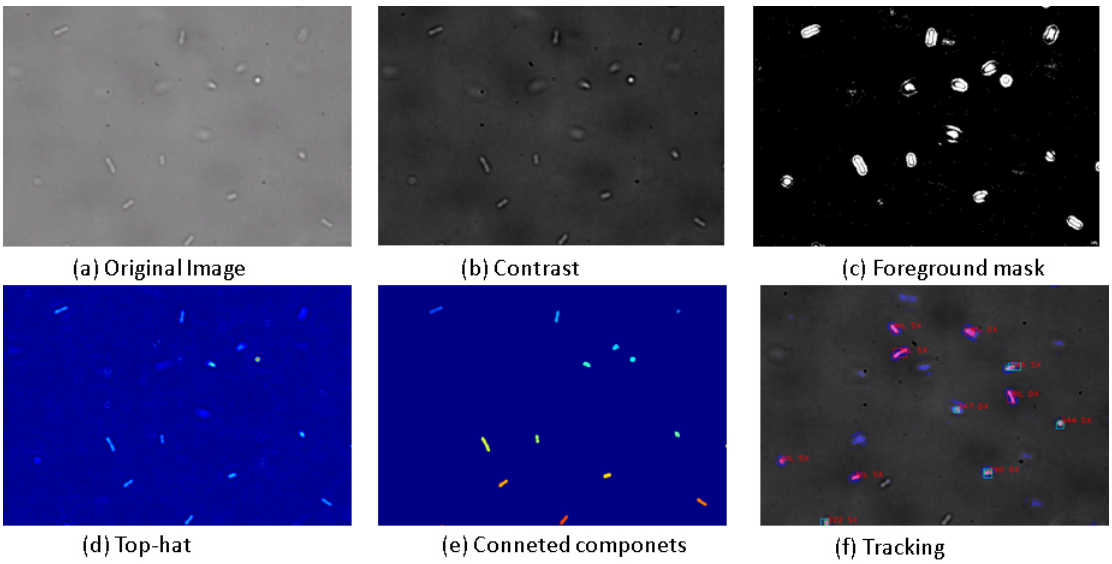

Fig. 5.19 The different phases of the tracking

The whole procedure is repeated for the entire image sequences taken during the lateral scan from bottom wall to top wall for various focal planes.

Chapter 6

Results and Discussion

This chapter summarizes the experimental results obtained concerning the study of the density distribution of bacterial solutions between two parallel walls. After a description of the experimental methodology developed for these experiments, we present the results for solutions of *E. coli* and *Pseudomonas*. For each type, we present and compare density profiles taken at different concentration and walls separation. Finally, we conclude by comparing the experimental scans with the preliminary results of a numerical model which considers only steric interactions among bacteria.

6.1 Experimental Methodology

The experiments were performed on two particular bacterial species, *Pseudomonas* and *E. coli*, that show different characteristics especially in terms of their propelling ability as discussed in chapter 3. Image acquisition was conducted according to the modalities described in chapter 5. In other words, we executed series of Z scans starting from the bottom wall to the top wall with varying step size. In order to have a better resolution, the step size was kept around 0.5 to 1 μm near the walls while in the middle the step was increased to 10 μm. At each position, 600 frames were taken at a frequency of 32fps. The spatial confinement chamber for image acquisition was realized in the following manner:

(a) Three liquid droplets were placed on the BSA treated glass plate as shown in figure 6.1. The middle drop represent bacterial solution (mixed with percoll) (figure 6.1 (a)), the two droplets on the side are distilled water (figure 6.1 (b)).

(b) The spacers (figure 6.1 (c)) were put on two distilled-water droplets (water droplets act as glue by capillarity).

(c) A second glass plate (treated with BSA) was placed over the spacer by putting two more drops of distilled-water.

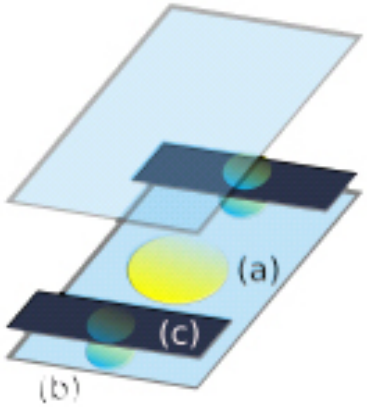

Fig. 6.1 A set-up of the sample preparation.

In our experiment we varied three parameters to systematically study the effect of spatial confinement which were:

(a) The type of bacteria.

(b) The separation between the glass plates .

(c) The density of the bacterial solution.

The bacterial cells tend to adhere to the glass plates due to the formation of bonds between the glass surface and pili or flagella of bacteria thereby preventing their movement. Hence, it was necessary to functionalize the glass plates before starting the experiment. For this purpose, a solution of Bovine Serum Albumin (BSA) was used which is well known for preventing adhesion. The functionalization was achieved by keeping the glass plates in a BSA solution for 15-20 hours. It can be observed from figure 6.2 that more bacteria adhere to the untreated glass plates as compared to the treated ones.

6.1.1 Image Analysis

In these experiments, the images were analyzed using the tracking software as described in chapter 5. The program needs a cutoff length D to distinguish between motile and non

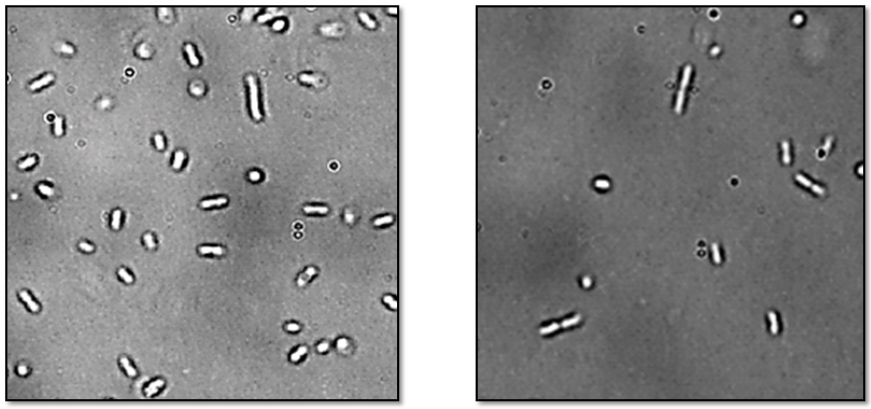

Fig. 6.2 The role of BSA. (a) Untreated glass plates. (b) Glass plates treated with BSA.

motile bacteria. More precisely, it analyzes all frames and tracks the centroids of the "slow" bacteria. If these move by a distance less than D over a typical time of $1/2$ sec, the bacteria is counted as passive. The active bacteria are then calculated by subtracting the number

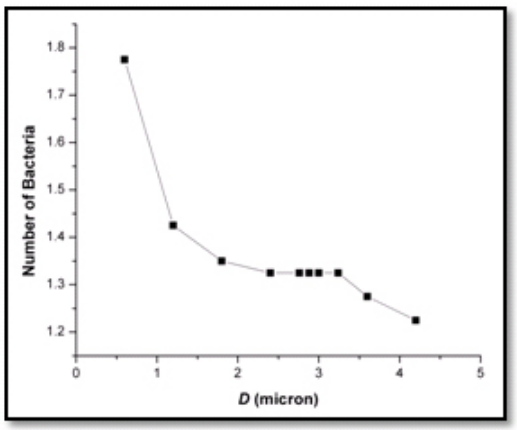

Fig. 6.3 Graphical representation of density distribution as a function of varying values of D.

of these passive particle from the total number of detected particles. Accordingly, if $D \geq W$, all particles are considered as passive, while if D is much smaller than the bacteria size all particles are taken as active. Figure 6.3 shows the number of motile *Pseudomonas* determined at the middle of a slit width of $W = 100\ \mu m$, by analyzing the same set of data as a function of the cutoff D. As expected, the number of active bacteria decreases with D. However, between 2.4 and 3.2 μm , there is a plateau suggesting that in this range the program outcome is insensitive on the actual value of D. In order to establish a criterium

for the choice of D we considered the mean square distance of a freely diffusing spherical particle in three dimensions which is given by:

$$\left\langle r^2 \right\rangle = 6D_{sphere}t$$

where D_{sphere} is the diffusion coefficient and t is the time in secs. D_{sphere} is given

$$D_{sphere} = \frac{K_B T}{6\pi\eta R_{eff}}$$

where k_B is the Boltzmann constant, T is the temperature, η is the viscosity of the medium and R_{eff} is the radius of the sphere. If we model as a first approximation the bacterium as a sphere of radius $\frac{l+b}{4}$, where $l \sim 2.5\ \mu m$ is the length of *E. coli* and $b \sim 0.8\ \mu m$ is its thickness. We get for *E. coli* a D_{sphere} close to $0.7\ \mu m^2/sec$. We notice that this mean distance is slightly below the lower limit of the plateau of figure 6.3. Furthermore, this is comparable to the length of bacteria. Accordingly in the data analysis we chose a value of D equal to the typical length of the bacteria i.e 2.5 μm for *E. coli* and 3 μm for *Pseudomonas*.

6.1.2 Buoyancy matching of the solution

The density difference between the growth medium and bacteria gives rise to sedimentation of bacteria towards the bottom glass plates due to gravity. This affects the measurement of the bacterial distribution as a function of position between the glass plates. In order to solve this problem, one needs to match the medium and bacteria buoyant density. A way to do this is to mix the bacterial solution with percoll. Percoll is considered to be a well-referenced medium for density matching fluid for cells, viruses, and subcellular particles as mentioned in chapter 5.

The correct value of percoll concentration was obtained by performing a series of density measurements with *E. coli* and *Pseudomonas* solutions at a fixed distance of 100 μm between bottom and the top wall. The matching condition was established by observing the symmetry in the density distribution profile of bacteria between the bottom and top walls of the glass plates. Figure 6.4 represent a series of density profiles taken at different concen-

tration of percoll, wherein the horizontal axis represents the distance from the bottom wall (Z) normalized to the slit width (W) and the vertical axis indicates the number of motile bacteria.

As it can be seen in Figure 6.4(a), a bacterial solution without percoll sedimented at the bottom wall due to gravity. However, gradual addition of percoll resulted in an increased density profile towards the top wall. At a percoll concentration of 40% (by volume) (figure 6.4(b)), an increased but non-symmetric distribution of bacteria at the top wall was observed. An addition of 50% - 60% percoll (by volume) to the bacterial solution (figure 6.4(c) and figure 6.4 (d)) led to symmetrical density profiles indicating a good density match.

Further increasing the percoll concentration to 70% (by volume) yielded an asymmetric profile with a higher density near the top wall (figure 6.4(e)). Accordingly, in all measurements we diluted the bacterial solutions with 50% of percoll.

6.1.3 Errors Estimate

The evaluation of the number of motile bacteria by the tracking software is prone to casual errors that depend on the choice of parameters which are somewhat subjective. These errors were estimated by comparing the results of analyses of the same set of experimental data done by different users. As an example, figure 6.5 shows the density profiles derived from the same raw images by two users who have selected different thresholds in the filters employed by the data imaging program. The two curves are slightly shifted. By carrying out extensive tests similar to these, we concluded that the number of active bacteria is estimated with an uncertainty of about 15%, a figure similar to that quoted in the original work by Berke et al. [2]

6.2 Measurement of density profiles

With the methodology previously described, we have measured the density profiles of bacterial solutions of different concentrations confined between two glass walls having a separation of 100, 150, 200, 250 μm.

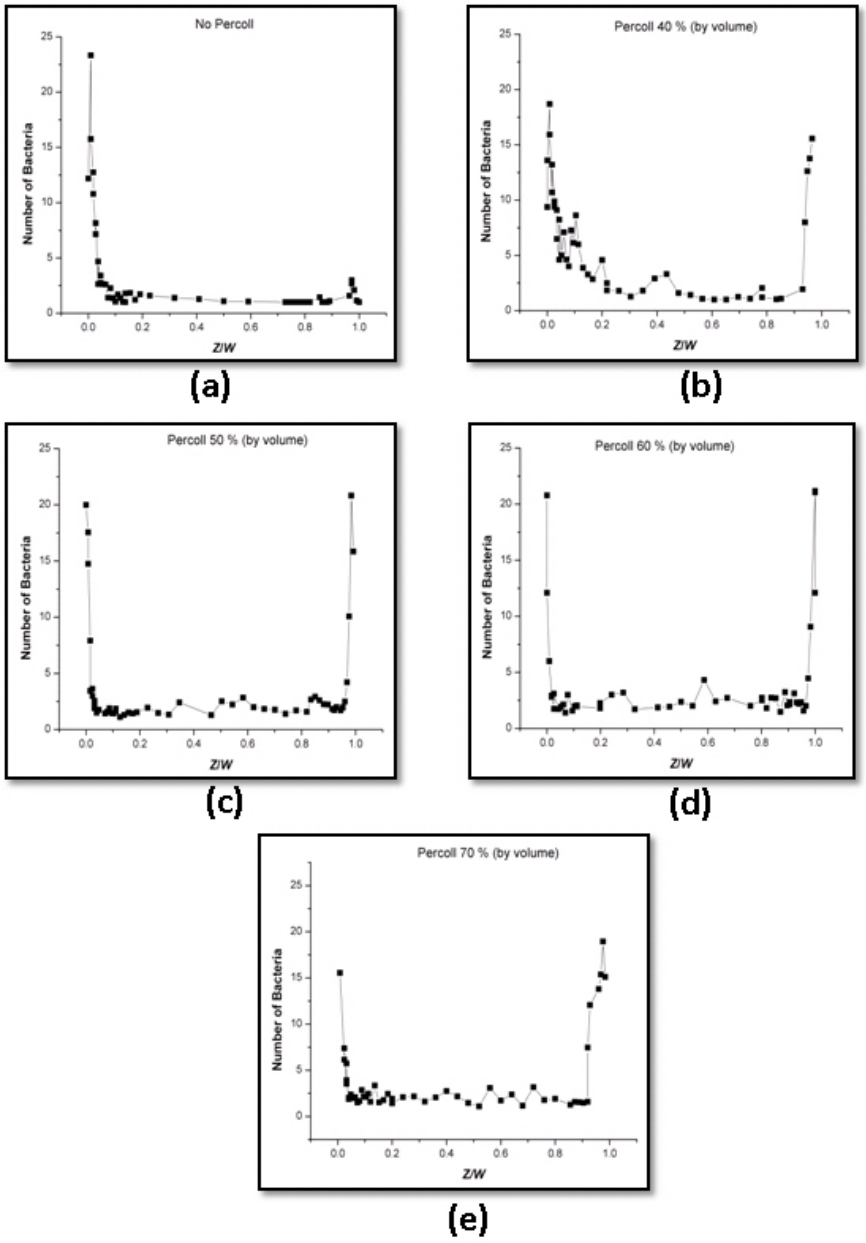

Fig. 6.4 Density profiles of bacterial solutions with different concentration of Percoll. The width between the two walls was kept constant at 100 μm.

Figure 6.6 shows the results obtained with a solution of *E. coli* with a concentration of $1.1 \cdot 10^8 cfu/ml$. The scans show a symmetric profile with a rapid enhancement close to the walls and in the middle a constant plateau where the density is constant and practically equal to its bulk density. This is in stark contrast with the behavior of passive particles (for instance dead bacteria) not interacting with the walls whose density profile is just flat. No

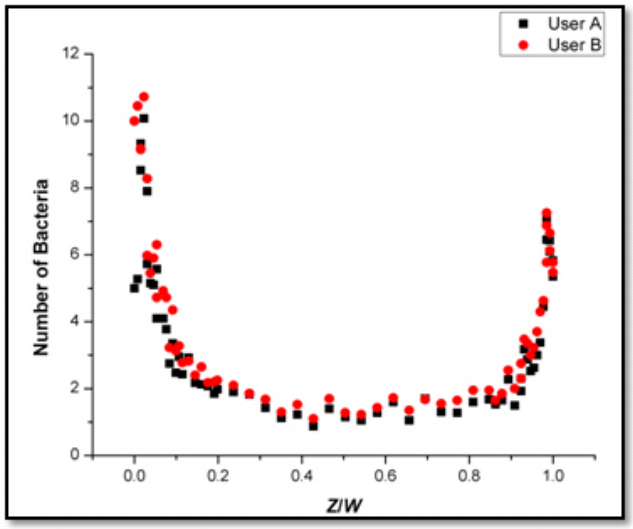

Fig. 6.5 Graph representing statistical errors determined by evaluation of density profile analyzed by different users.

apparent difference can be noticed among the 5 scans. To make sure that the measurements were not affected by a variation of the number density of the solution, at the end of the data acquisition we repeated the initial scan with $W = 100\ \mu m$. Again, no apparent difference can be noticed between these two scans, which were taken after 6 hours, suggesting that the solution barely changed during the measurement. This was confirmed by the optical density measurements carried out at the end of the data campaign which yielded a value of $1.3 \cdot 10^8 cfu/ml$, practically coincident with the initial value. Figure 6.7 shows the sequence of scans taken at a much larger concentration of *E. coli*. Again, the profiles present the same overall behavior already discussed and no systematic differences can be distinguished at varying W. We have then compared the density profiles with $W = 150\ \mu m$ taken at the two concentrations. Figure 6.8 compares two curves, where that at low concentration has been obtained by multiplying the original data in figure 6.6 by a constant factor of 3.2. This factor is about half the ratio between the two nominal bulk concentrations. We do not know the reason of such discrepancy. Systematic studies are under way to clarify this point. Notwithstanding, a conclusion we can draw from the *E. coli* measurement is that the observed enhancement at the wall does not seem to be affected by either solution concentration or the confining width. This latter result in contradiction with the numerical simulation

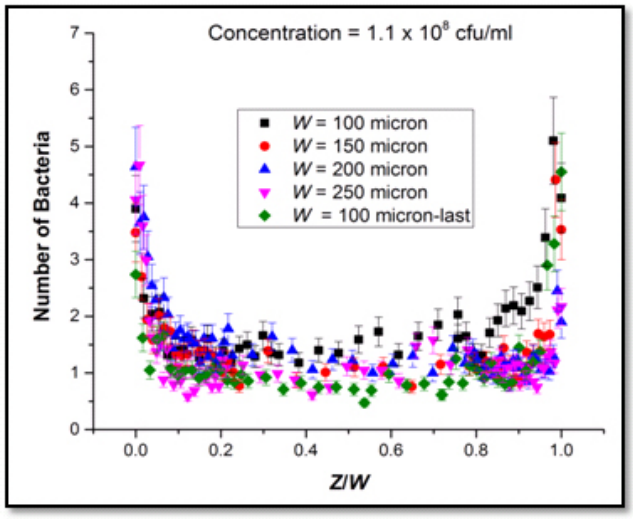

Fig. 6.6 Number of active *E. coli* as a function of distance from bottom wall Z.

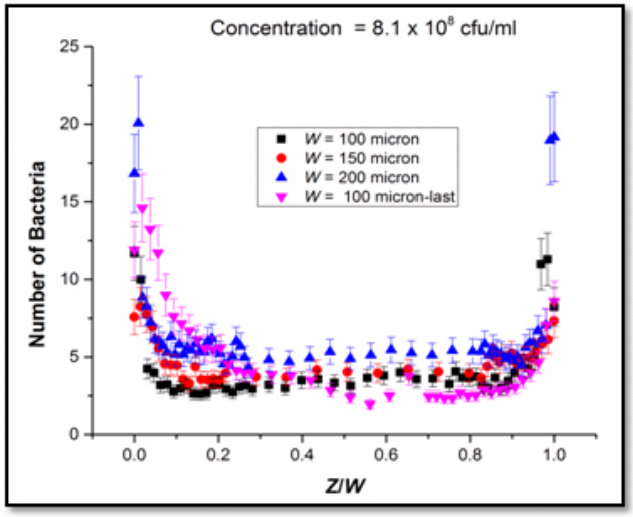

Fig. 6.7 Number of active *E. coli* as a function of distance from bottom wall Z.

presented in chapter 4, figure 4.8. However, we need to point out that the simulation results refer to much smaller widths than those used in the measurements. Overall, this suggests that important confining effects can be observed at distances smaller than about 50 μm.

We have repeated these measurements with *Pseudomonas*, an aerobic bacteria which has a propulsion mechanism different from that of *E. coli* (see chapter 3). Figures 6.9 and 6.10 show the profiles scans taken at two different solution concentrations. Again, there is no systematic observable difference among the various scans. As before, figure 6.11

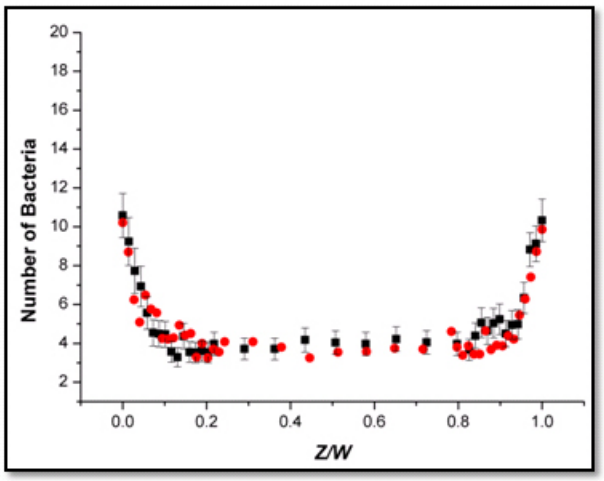

Fig. 6.8 Number of active *E. coli* as a function of distance from bottom wall Z, the black dots represent the density of *E. coli* at higher concentration whereas red dots represent density of *E. coli* at lower concentration multiplied by a constant factor of 3.2

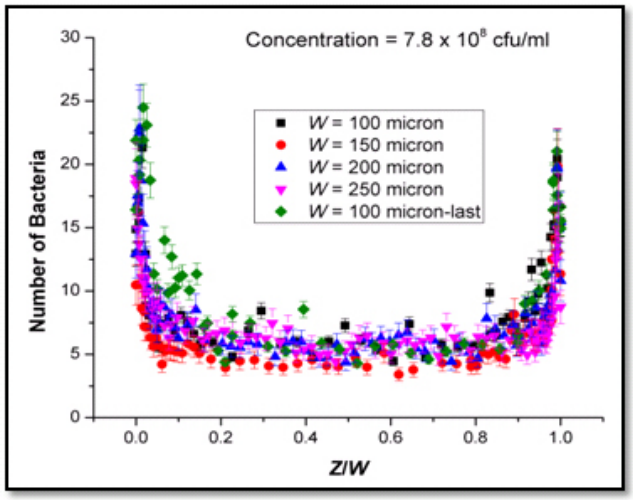

Fig. 6.9 Number of active *Pseudomonas* as a function of distance from bottom wall Z.

compares the density profiles of *Pseudomonas* for a slit width of $W = 150\ \mu m$ taken at the two different concentrations. No variation is discernible between the scan at higher concentration and that at lower concentration multiplied by a factor of 1.1. Finally figure 6.12 shows the comparison of *E. coli* and *Pseudomonas* scans taken at $W = 200\ \mu m$ and concentration of about $8 \cdot 10^8 cfu/ml$. The good agreement between the two profiles clearly suggests that the phenomenon of density enhancement at the walls does not depend on the motility mechasism of the bacteria.

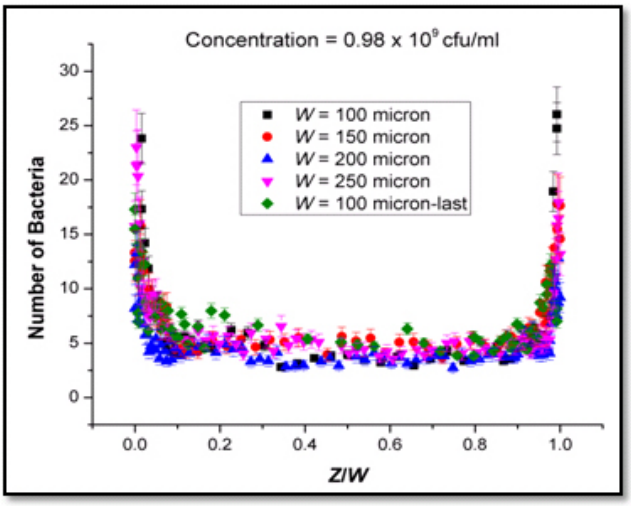

Fig. 6.10 Number of active *Pseudomonas* as a function of distance from bottom wall Z.

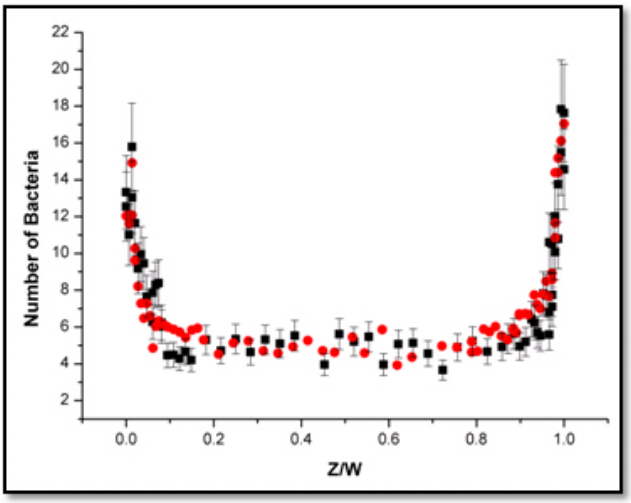

Fig. 6.11 Number of active *Pseudomonas* as a function of distance from bottom wall Z, the black dots represent the density of *Pseudomonas* at higher concentration whereas red dots represent density of *Pseudomonas* at lower concentration multiplied by a constant factor of 1.1

6.3 Determination of motility speed of bacteria

The numerical simulations require as an input the particle motility. We have determined the characteristic values of the two species used by tracking the trajectories of several bacteria. This was accomplished by focusing the objective at a distance close to the (bottom) wall, because in this region the bacteria move preferentially in a direction parallel to the wall. A

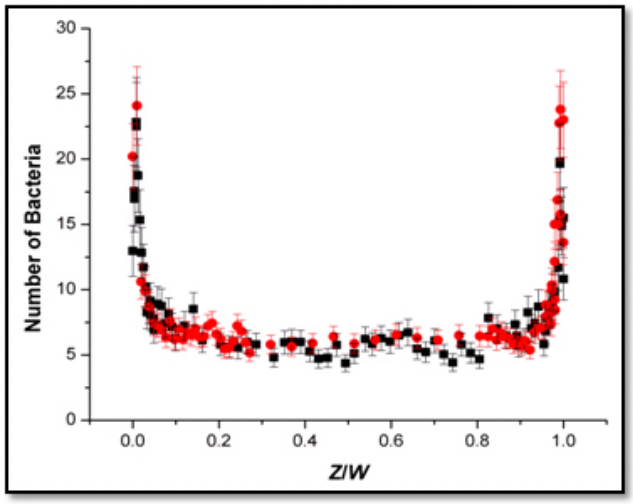

Fig. 6.12 A comparison of *E. coli* and *Pseudomonas*. Black dots represent *Pseudomonas* whereas red dots correspond to *E. coli* multiplied with a constant factor of 1.2

sequence of images was then taken at a frequency of 32Hz. With the help of Nikon-NIS software, it was possible to reconstruct the trajectories of bacteria which were moving in focus during the acquisition time. Figure 6.13 displays four typical trajectories, which were obtained by overlapping about 20-25 consecutive frames. For each trajectories an average speed could be derived. By averaging the values derived from about 10 of these trajectories

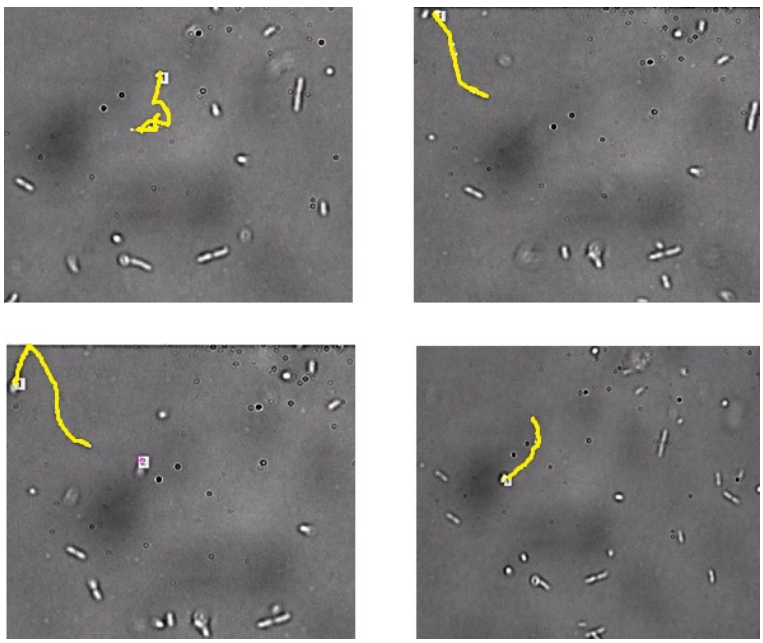

Fig. 6.13 Microscopic view for different path trajectories of bacteria.

we came up with a mean speed of $25\mu/sec$ for *E. coli* and of 35 μ/sec *Pseudomonas* which are in agreement with the values found in the literature [71]

6.4 Comparison of experimental and simulation results:

We have compared our experimental data with the preliminary simulation results as discussed in chapter 4. The simulation was performed for 100 self propelled particles (N_a) confined between the two square walls having a side of 200 μm and a separation of 100 μm. This would correspond to a volume density of $0.25 \cdot 10^8 cfu/ml$. Figure 6.14 shows a quantitative comparison with the experimental data of *Pseudomonas* having a concentration of about $7.1 \cdot 10^8 cfu/ml$ for a slit width of 100 μm.

The two curves show a nice agreement, where the numerical data have been multiplied by a factor of 3.5. This contrasts with the ratio between the two nominal bluk densities. We do not know the reason of such a discrepancy. Tests are under way to evaluate the program outcome. Apart from this, the similar trend between the experimental and preliminary simu-

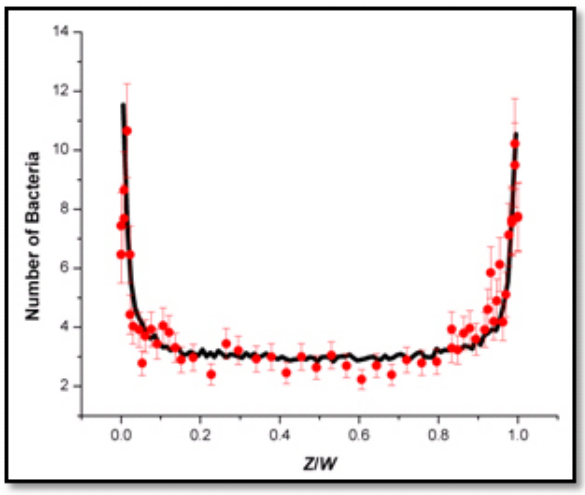

Fig. 6.14 Comparison of experimental results with simulation results. The solid line represents simulation results multiplied by a constant factor of 3.5 and red dots corresponds to the experimental values

lation results suggests that steric interactions and motility determine the spatial distribution of bacteria. It is not necessary to invoke the action of hydrodynamic interaction to explain

the experimental observation as was original done by Berke et al. [2]. The simple alignment of rod-shaped bacteria parallel to the wall due to steric interaction is sufficient to reproduce the density enhancement at the walls.

Chapter 7

Conclusions

In this thesis we have carried out a systematic study of the spatial confinement of the bacterial communities. Solutions of *E. coli* and *Pseudomonas* of known concentration were prepared by standard microbiology techniques. In the experiments they were confined between two glass walls having a sub-millmetric separation.

The distribution of bacteria within the slit was investigated by optical microscopy. The detection of motile bacteria was done by a custom made tracking software. In this way, we measured the density profiles of the two species at varying solution concentration (N) and wall separation (W). They present an enhancement at the walls.

In the agreement with pervious studies. Furthermore, they suggest that this phenomenon is not affected by either (N) or (W), at least for the parameter values investigated. A comparison with preliminary results of a statistical model indicates that this effect is mainly caused by steric interactions among the bacteria.

The whole methodology developed for this study, which was mostly new for the research groups involved in the project can be extended to the dynamic phenomena. In particular, the study of the transport properties of bacterial solutions, both one and two components, in microchannels under the action of varying pressure gradients. Novel non-linear phenomena are expected.

References

[1] G. Li and J. X. Tang, "Accumulation of microswimmers near a surface mediated by collision and rotational brownian motion," Physical Review Letters **103**, 078101 (2009).

[2] A. P. Berke, L. Turner, H. C. Berg, and E. Lauga, "Hydrodynamic attraction of swimming microorganisms by surfaces," Physical Review Letters **101**, 038102 (2008).

[3] T. Vicsek and A. Zafeiris, "Collective motion," Physics Reports **517**, 71–140 (2012).

[4] G. I. Menon, "Active matter," pp. 193–218 (2010).

[5] F. Jülicher, A. Ajdari, and J. Prost, "Modeling molecular motors," Reviews of Modern Physics **69**, 1269 (1997).

[6] E. M. Purcell, "Life at low reynolds number," Am. J. Phys **45**, 3–11 (1977).

[7] J. R. Howse, R. A. Jones, A. J. Ryan, T. Gough, R. Vafabakhsh, and R. Golestanian, "Self-motile colloidal particles: from directed propulsion to random walk," Physical Review Letters **99**, 048102 (2007).

[8] H.-R. Jiang, N. Yoshinaga, and M. Sano, "Active motion of a janus particle by self-thermophoresis in a defocused laser beam," Physical Review Letters **105**, 268302 (2010).

[9] J. L. Anderson, "Colloid transport by interfacial forces," Annual Review of Fluid Mechanics **21**, 61–99 (1989).

[10] S. Ramaswamy, "The mechanics and statistics of active matter," The Mechanics and Statistics of Active Matter **1**, 323–345 (2010).

[11] S. Rice, A. W. Lin, D. Safer, C. L. Hart, N. Naber, B. O. Carragher, S. M. Cain, E. Pechatnikova, E. M. Wilson-Kubalek, M. Whittaker *et al.*, "A structural change in the kinesin motor protein that drives motility," Nature **402**, 778–784 (1999).

[12] W. R. Schief and J. Howard, "Conformational changes during kinesin motility," Current opinion in cell biology **13**, 19–28 (2001).

[13] M. Cates, D. Marenduzzo, I. Pagonabarraga, and J. Tailleur, "Arrested phase separation in reproducing bacteria creates a generic route to pattern formation," Proceedings of the National Academy of Sciences **107**, 11715–11720 (2010).

[14] H. H. Wensink, J. Dunkel, S. Heidenreich, K. Drescher, R. E. Goldstein, H. Löwen, and J. M. Yeomans, "Meso-scale turbulence in living fluids," Proceedings of the National Academy of Sciences **109**, 14308–14313 (2012).

[15] J. Dunkel, S. Heidenreich, K. Drescher, H. H. Wensink, M. Bär, and R. E. Goldstein, "Fluid dynamics of bacterial turbulence," Physical Review Letters **110**, 228102 (2013).

[16] A. Baskaran and M. C. Marchetti, "Statistical mechanics and hydrodynamics of bacterial suspensions," Proceedings of the National Academy of Sciences **106**, 15567–15572 (2009).

[17] H. R. Brand, H. Pleiner, and F. Ziebert, "Macroscopic dynamics of polar nematic liquid crystals," Physical Review E **74**, 021713 (2006).

[18] K. Anderson, Y.-L. Wang, and J. Small, "Coordination of protrusion and translocation of the keratocyte involves rolling of the cell body." The Journal of cell biology **134**, 1209–1218 (1996).

[19] R. Poincloux, O. Collin, F. Lizárraga, M. Romao, M. Debray, M. Piel, and P. Chavrier, "Contractility of the cell rear drives invasion of breast tumor cells in 3d matrigel," Proceedings of the National Academy of Sciences **108**, 1943–1948 (2011).

[20] G. Salbreux, J. Prost, and J. Joanny, "Hydrodynamics of cellular cortical flows and the formation of contractile rings," Physical Review Letters **103**, 058102 (2009).

[21] P. Friedl and K. Wolf, "Tumour-cell invasion and migration: diversity and escape mechanisms," Nature Reviews Cancer **3**, 362–374 (2003).

[22] M. Ballerini, N. Cabibbo, R. Candelier, A. Cavagna, E. Cisbani, I. Giardina, A. Orlandi, G. Parisi, A. Procaccini, M. Viale *et al.*, "Empirical investigation of starling flocks: a benchmark study in collective animal behaviour," Animal behaviour **76**, 201–215 (2008).

[23] J. W. Bradbury and S. L. Vehrencamp, *Principles of animal communication* (1998).

[24] K. Drescher, J. Dunkel, L. H. Cisneros, S. Ganguly, and R. E. Goldstein, "Fluid dynamics and noise in bacterial cell–cell and cell–surface scattering," Proceedings of the National Academy of Sciences **108**, 10940–10945 (2011).

[25] L. Angelani, R. Di Leonardo, and G. Ruocco, "Self-starting micromotors in a bacterial bath," Physical Review Letters **102**, 048104 (2009).

[26] R. Di Leonardo, L. Angelani, D. Dell'Arciprete, G. Ruocco, V. Iebba, S. Schippa, M. Conte, F. Mecarini, F. De Angelis, and E. Di Fabrizio, "Bacterial ratchet motors," Proceedings of the National Academy of Sciences **107**, 9541–9545 (2010).

[27] R. P. Feynman, J. Hey, and R. W. Allen, *Feynman lectures on computation* (Addison-Wesley Longman Publishing Co., Inc., 1998).

[28] H. C. Berg and L. Turner, "Chemotaxis of bacteria in glass capillary arrays. escherichia coli, motility, microchannel plate, and light scattering," Biophysical Journal **58**, 919–930 (1990).

[29] G. Li, L.-K. Tam, and J. X. Tang, "Amplified effect of brownian motion in bacterial near-surface swimming," Proceedings of the National Academy of Sciences **105**, 18355–18359 (2008).

[30] L. Rothschild, "Structure and movements of tick spermatozoa (arachnida, acari)," Quarterly Journal of Microscopical Science **3**, 239–247 (1961).

[31] H. Winet, G. Bernstein, and J. Head, "Observations on the response of human spermatozoa to gravity, boundaries and fluid shear," Journal of reproduction and fertility **70**, 511–523 (1984).

[32] P. D. Frymier and R. M. Ford, "Analysis of bacterial swimming speed approaching a solid–liquid interface," AIChE journal **43**, 1341–1347 (1997).

[33] J. Männik, R. Driessen, P. Galajda, J. E. Keymer, and C. Dekker, "Bacterial growth and motility in sub-micron constrictions," Proceedings of the National Academy of Sciences **106**, 14861–14866 (2009).

[34] W. R. DiLuzio, L. Turner, M. Mayer, P. Garstecki, D. B. Weibel, H. C. Berg, and G. M. Whitesides, "Escherichia coli swim on the right-hand side," Nature **435**, 1271–1274 (2005).

[35] S. E. Spagnolie and E. Lauga, "Hydrodynamics of self-propulsion near a boundary: predictions and accuracy of far-field approximations," Journal of Fluid Mechanics **700**, 105–147 (2012).

[36] P. D. Frymier, R. M. Ford, H. C. Berg, and P. T. Cummings, "Three-dimensional tracking of motile bacteria near a solid planar surface," Proceedings of the National Academy of Sciences **92**, 6195–6199 (1995).

[37] H. Shum, E. Gaffney, and D. Smith, "Modelling bacterial behaviour close to a no-slip plane boundary: the influence of bacterial geometry," Proceedings of the Royal Society A: Mathematical, Physical and Engineering Science p. rspa20090520 (2010).

[38] J. Elgeti and G. Gompper, "Self-propelled rods near surfaces," EPL (Europhysics Letters) **85**, 38002 (2009).

[39] G. Li, J. Bensson, L. Nisimova, D. Munger, P. Mahautmr, J. X. Tang, M. R. Maxey, and Y. V. Brun, "Accumulation of swimming bacteria near a solid surface," Physical Review E **84**, 041932 (2011).

[40] E. Lauga, W. R. DiLuzio, G. M. Whitesides, and H. A. Stone, "Swimming in circles: motion of bacteria near solid boundaries," Biophysical journal **90**, 400–412 (2006).

[41] S. E. Hulme, W. R. DiLuzio, S. S. Shevkoplyas, L. Turner, M. Mayer, H. C. Berg, and G. M. Whitesides, "Using ratchets and sorters to fractionate motile cells of escherichia coli by length," Lab on a Chip **8**, 1888–1895 (2008).

[42] J. v. Zuylen, "The microscopes of antoni van leeuwenhoek," Journal of microscopy **121**, 309–328 (1981).

[43] B. Amos, "Lessons from the history of light microscopy," Nature cell biology **2**, E151–E152 (2000).

[44] N. This, "National institutes of health consensus development conference statement: management of hepatitis c: 2002—june 10-12, 2002," Management **2002** (2002).

[45] J. Willey, *Prescott, Harley, and Klein's Microbiology-7th international ed./Joanne M. Willey, Linda M. Sherwood, Christopher J. Woolverton* (New York [etc.]: McGraw-Hill Higher Education, 2008).

[46] P. R. Murray, W. L. Drew, G. S. Kobayashi, J. Thompson Jr *et al.*, *Medical microbiology.* (Wolfe Medical Publications Ltd, 1990).

[47] E. Jawetz, J. L. Melnick, and E. A. Adelberg, "Review of medical microbiology," (1980).

[48] M. Alexander *et al.*, *Introduction to soil microbiology.*, Ed. 2 (John Wiley & Sons., 1977).

[49] M. T. Madigan, J. M. Martinko, J. Parker, and T. D. Brock, *Biology of microorganisms*, vol. 985 (prentice hall Upper Saddle River, NJ, 1997).

[50] L. Gan, S. Chen, and G. J. Jensen, "Molecular organization of gram-negative peptidoglycan," Proceedings of the National Academy of Sciences **105**, 18953–18957 (2008).

[51] M. Bayer, "Areas of adhesion between wall and membrane of escherichia coli," Journal of general microbiology **53**, 395–404 (1968).

[52] M. Wheelis, *Principles of modern microbiology* (Jones & Bartlett Publishers, 2011).

[53] G. B. Johnson, G. J. Brusca, and R. Holt, *Biology, visualizing life* (Holt, Rinehart and Winston Austin, 1994).

[54] C. Branden, J. Tooze *et al.*, *Introduction to protein structure*, vol. 2 (Garland New York, 1991).

[55] B. Eddy, "The use and meaning of the term 'psychrophilic'," Journal of Applied Bacteriology **23**, 189–190 (1960).

[56] P. H. Sneath, "Some thoughts on bacterial classification," Journal of general microbiology **17**, 184–200 (1957).

[57] H. C. Berg, *E. coli in Motion* (Springer, 2004).

[58] H. O. M. Al-Dahmoshi, "Genotypic and phenotypic investigation of alginate biofilm formation among pseudomonas aeruginosa isolated from burn victims in babylon, iraq," Science Journal of Microbiology **2013** (2013).

[59] T. Strateva and D. Yordanov, "Pseudomonas aeruginosa–a phenomenon of bacterial resistance," Journal of medical microbiology **58**, 1133–1148 (2009).

[60] S. A. Ochoa, F. López-Montiel, G. Escalona, A. Cruz-Córdova, L. B. Dávila, B. López-Martínez, Y. Jiménez-Tapia, S. Giono, C. Eslava, R. Hernández-Castro *et al.*, "Pathogenic characteristics of pseudomonas aeruginosa strains resistant to carbapenems associated with biofilm formation," Bol Med Hosp Infant Mex **70**, 133–144 (2013).

[61] E. Drenkard and F. M. Ausubel, "Pseudomonas biofilm formation and antibiotic resistance are linked to phenotypic variation," Nature **416**, 740–743 (2002).

[62] M. Zwietering, I. Jongenburger, F. Rombouts, and K. Van't Riet, "Modeling of the bacterial growth curve," Applied and environmental microbiology **56**, 1875–1881 (1990).

[63] R. M. Macnab and S.-I. Aizawa, "Bacterial motility and the bacterial flagellar motor," Annual review of biophysics and bioengineering **13**, 51–83 (1984).

[64] M. Li, "Experimental study of swimming flagellated bacteria and their collective behaviour in concentrated suspensions," (2010).

[65] R. M. Harshey, "Bacterial motility on a surface: many ways to a common goal," Annual Reviews in Microbiology **57**, 249–273 (2003).

[66] H. C. Berg and R. A. Anderson, "Bacteria swim by rotating their flagellar filaments," (1973).

[67] Y. Magariyama, S. Sugiyama, and S. Kudo, "Bacterial swimming speed and rotation rate of bundled flagella," FEMS microbiology letters **199**, 125–129 (2001).

[68] H. C. Berg, D. A. Brown *et al.*, "Chemotaxis in escherichia coli analysed by three-dimensional tracking," Nature **239**, 500–504 (1972).

[69] S. Chattopadhyay, R. Moldovan, C. Yeung, and X. Wu, "Swimming efficiency of bacterium escherichiacoli," Proceedings of the National Academy of Sciences **103**, 13712–13717 (2006).

[70] K. J. Duffy and R. M. Ford, "Turn angle and run time distributions characterize swimming behavior for pseudomonas putida." Journal of bacteriology **179**, 1428–1430 (1997).

[71] T. B. Doyle, A. C. Hawkins, and L. L. McCarter, "The complex flagellar torque generator of pseudomonas aeruginosa," Journal of bacteriology **186**, 6341–6350 (2004).

[72] D. B. Kearns, "A field guide to bacterial swarming motility," Nature Reviews Microbiology **8**, 634–644 (2010).

[73] J. Liu and J. S. Parkinson, "Genetic evidence for interaction between the chew and tsr proteins during chemoreceptor signaling by escherichia coli." Journal of bacteriology **173**, 4941–4951 (1991).

[74] J. E. Segall, M. D. Manson, and H. C. Berg, "Signal processing times in bacterial chemotaxis," Nature **296**, 855–857 (1982).

[75] C. Storm, J. J. Pastore, F. C. MacKintosh, T. C. Lubensky, and P. A. Janmey, "Nonlinear elasticity in biological gels," Nature **435**, 191–194 (2005).

[76] T. Surrey, F. Nédélec, S. Leibler, and E. Karsenti, "Physical properties determining self-organization of motors and microtubules," Science **292**, 1167–1171 (2001).

[77] T. Vicsek, A. Czirók, E. Ben-Jacob, I. Cohen, and O. Shochet, "Novel type of phase transition in a system of self-driven particles," Physical review letters **75**, 1226 (1995).

[78] A. Sokolov, I. S. Aranson, J. O. Kessler, and R. E. Goldstein, "Concentration dependence of the collective dynamics of swimming bacteria," Physical Review Letters **98**, 158102 (2007).

[79] R. Albert and A.-L. Barabási, "Statistical mechanics of complex networks," Reviews of modern physics **74**, 47 (2002).

[80] H. Chaté, F. Ginelli, G. Grégoire, F. Peruani, and F. Raynaud, "Modeling collective motion: variations on the vicsek model," The European Physical Journal B-Condensed Matter and Complex Systems **64**, 451–456 (2008).

[81] M. Aldana, V. Dossetti, C. Huepe, V. Kenkre, and H. Larralde, "Phase transitions in systems of self-propelled agents and related network models," Physical Review Letters **98**, 095702 (2007).

[82] G. Baglietto and E. V. Albano, "Nature of the order-disorder transition in the vicsek model for the collective motion of self-propelled particles," Physical Review E **80**, 050103 (2009).

[83] D. Saintillan, "The dilute rheology of swimming suspensions: A simple kinetic model," Experimental Mechanics **50**, 1275–1281 (2010).

[84] D. J. Sumpter, *Collective animal behavior* (Princeton University Press, 2010).

[85] D. J. Stephens and V. J. Allan, "Light microscopy techniques for live cell imaging," Science **300**, 82–86 (2003).

[86] E. Hecht and A. Zajac, "Optics," (1974).

[87] D. Gabor *et al.*, "A new microscopic principle," Nature **161**, 777–778 (1948).

[88] G. O. Reynolds, J. B. Develis, G. B. Parrent, and B. Thompson, "The new physical optics notebook: tutorials in fourier optics," **61** (1989).

[89] M. Born and E. Wolf, "Principles of optics: electromagnetic theory of propagation, interference and diffraction of light," (1999).

[90] E. Ash and G. Nicholls, "Super-resolution aperture scanning microscope," (1972).

[91] D. B. Schmolze, C. Standley, K. E. Fogarty, and A. H. Fischer, "Advances in microscopy techniques," Archives of pathology & laboratory medicine **135**, 255–263 (2011).

[92] L. Bertucco, G. Nunnari, C. Randieri, V. Rizza, and A. Sacco, "A cellular neural network based system for cell counting in culture of biological cells," **1**, 341–345 (1998).

[93] E. Rosenberg, K. H. Keller, and M. Dworkin, "Cell density-dependent growth of myxococcus xanthus on casein." Journal of Bacteriology **129**, 770–777 (1977).

[94] F. Widdel, "Theory and measurement of bacterial growth," Di dalam Grundpraktikum Mikrobiologie **4** (2007).

[95] K. Fuwa and B. Valle, "The physical basis of analytical atomic absorption spectrometry. the pertinence of the beer-lambert law." Analytical Chemistry **35**, 942–946 (1963).

[96] D. Swinehart, "The beer-lambert law," Journal of chemical education **39**, 333 (1962).

[97] A. Fernandez-Barbero, A. Fernandez-Nieves, I. Grillo, and E. Lopez-Cabarcos, "Structural modifications in the swelling of inhomogeneous microgels by light and neutron scattering," Physical Review E **66**, 051803 (2002).

[98] E. Molina Grima, F. García Camacho, J. Sánchez Pérez, F. Acién Fernández, and J. Fernández Sevilla, "Evaluation of photosynthetic efficiency in microalgal cultures using averaged irradiance," Enzyme and microbial technology **21**, 375–381 (1997).

[99] C. W. Park, K. Y. Yoon, J. H. Byeon, K. Kim, and J. Hwang, "Development of rapid assessment method to determine bacterial viability based on ultraviolet and visible (uv-vis) spectroscopy analysis including application to bioaerosols," Aerosol and Air Quality Research **12**, 399–408 (2012).

[100] J. Adler and B. Templeton, "The effect of environmental conditions on the motility of escherichia coli," Journal of general microbiology **46**, 175–184 (1967).

[101] A. Biosciences, "Percoll methodology and applications. amersham biosciences," (2001).

[102] R. Bhalla, Q. Chen, Q. Cheng, N. Pandey, P. E. Rouviere, K. Ruebling-Jass, and A. Sachan, "Recombinant host cells having an increase in buoyant density," (2011). US Patent App. 13/164,990.

[103] C. Solà, R. Cristòfol, C. Suñol, and C. Sanfeliu, "Primary cultures for neurotoxicity testing," pp. 87–103 (2011).

[104] M. D. Hoover, G. L. Finch, and B. T. Castorina, "Sodium metatungstate as a medium for measuring particle density using isopycnic density gradient ultracentrifugation," Journal of Aerosol Science **22**, 215–221 (1991).

[105] D. A. Forsyth and J. Ponce, "Computer vision: a modern approach," (2002).

[106] G. R. Bradski, "Computer vision face tracking for use in a perceptual user interface," (1998).

[107] G. Bradski and A. Kaehler, "Learning opencv: Computer vision with the opencv library," (2008).